EPSC2018

TP6/SB21 abstracts

EPSC Abstracts
Vol. 12, EPSC2018-33, 2018
European Planetary Science Congress 2018

Corkscrew Flow Motion of Planetary Ions in the Venus Plasma Wake

H. Pérez-de-Tejada [(1),] R. Lundin [(2)], (1) Institute of Geophysics, UNAM, México, D. F; (2) Swedish Institute of Space Physics, Kiruna, Sweden

Measurements conducted with the Venus Express spacecraft (VEX) have led to the detection of a vortex structure in the Venus plasma wake. The scale size of that feature together with the local speed of ions in the vortex and values of the kinematic viscosity coefficient of the solar wind provide an estimate of the swirl period of the vortex. Comparative values of the speed of the particles produced by the period of the vortex and also their speed along the wake axis lead to a corkscrew shape for their motion as they move downstream from Venus. The flow streamlines are warped up within the wake and are oriented at a rate that varies with the solar wind conditions. Calculations show that the orientation of the flow streamlines along the corkscrew is dictated by the local value of the Reynolds number R given by the speed of the solar wind and the scale size of the vortex. At values of the Reynolds number smaller than those inferred from the VEX measurements the flow streamlines will be more warped up along the corkscrew. The opposite will occur at larger values of the Reynolds number.

VEX DATA

An overall description of a vortex structure measured in the Venus wake is reproduced in **Figure 1.** The orientation of the velocity vectors of H+ ions on the YZ plane transverse to the sun-Venus direction is shown in the upper panel). Their orientation along the X-axis in cylindrical coordinates is indicated in lower panel. The distribution of the velocity vectors is consistent with the presence of a vortex structure that extends across most of the Venus wake and that leads to a return flow in its central region directed back to Venus [1, 2]. The magnitude of the velocity vectors directed towards positive Y values at the top of the lower panel is larger than those of the velocity vectors closer to the wake axis. This difference implies the presence of a velocity boundary layer across the wake with velocity vectors directed back to Venus in the central part.

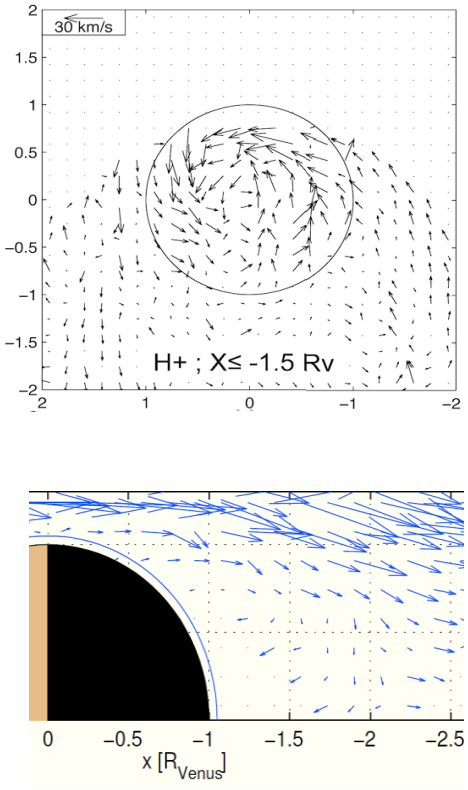

Figure 1 (upper panel) Velocity vectors of 1 - 300 eV H+ ions measured with the VEX spacecraft in the Venus near wake projected on the YZ plane transverse to the solar wind direction (Y and Z are the horizontal and the vertical axis). Data are averaged in 1000 x 1000 km columns at X < -1.5 R_V (1). (lower panel) Average direction of solar wind ion velocity vectors across the Venus near wake collected from many VEX orbits and projected in cylindrical coordinates (2).

The vorticity equation

The vorticity (Helmholtz) equation of a rotational flow (3) is:

$$\partial \boldsymbol{\omega}/\partial t = \nabla \times (\mathbf{V} \times \boldsymbol{\omega}) + \nu \nabla^2 \omega \qquad (1)$$

where the first term in the right side states changes of the vorticity vector $\boldsymbol{\omega} = \nabla \times \mathbf{V}$ produced by its own convection, and the second term is related to diffusion processes. **V** is the velocity vector of the flow, and ν is its kinematic viscosity coefficient. In dimensional form for incompressible fluids equation (1) can be reduced to:

$$\omega/T = U\,\omega/L + \boldsymbol{\nu}\,\omega/L^2 \qquad (2)$$

where U is the dominant speed of the flow and L the scale length of the vortex within the flow.

In terms of the Reynolds number R = UL/**ν** this equation is in turn:

$$T = RT^*/(1 + R) \qquad (3)$$

where T = L/U is the travel time of a flow parcel around the vortex structure and T* is that for very small values of the kinematic viscosity coefficient.

Using L = 6000 km as the scale size of the average vortex reproduced in Figure 1 and by taking U = 30 km/s as the speed limit of the H+ ions in the Venus wake shown in Figure 1we can first derive T* = 200 s as an approximate value for the travel time of a fluid parcel on a distance πL around the vortex for the limiting case of very small kinematic viscosity coefficient values (R → ∞) More representative calculations can be conducted by employing values of the order of $\nu \sim (10^3 - 10^5)$ km^2/s for the lower and upper order of magnitude of the kinematic viscosity coefficient [4]. With these numbers we are led to R ~ 180 – 1.8 for the Reynolds number leading to the values for the swirl period of the vortex presented in **Table 1.**

υ	**Reynolds Number**	**Rotation Period**
	∞	200 s
10^3 km^2/s	180	198 s
10^4 km^2/s	18	189 s
10^5 km^2/s	1.8	128 s
∞	0	0 s

Table 1 (left column) Nominal values of the kinematic viscosity coefficient υ of the solar wind. (middle-right columns) Values of the Reynolds number and the rotation period for the vortex in the upper panel of Figure 1.

The corkscrew flow in the O+ ion streamlines

The effect of adding the ion motion along the vortex to their velocity component along the wake axis will produce a torque in the manner that they are displaced thus leading to a corkscrew shape in their displacement as it is illustrated in **Figure 2**. Even though the shape of the flow motion in **Figure 1** corresponds to average conditions the warping of the flow streamlines will vary depending on the solar wind speed and the scale size of the vortex. Smaller values of the Reynolds number R in equation (3) will lead to smaller values of the rotation period thus increasing the particles rotation speed around the vortex in order to complete each turn. Under such conditions the flow streamlines in the corkscrew diagram will be more warped up than that predicted from the measured values. With larger R values the opposite will occur.

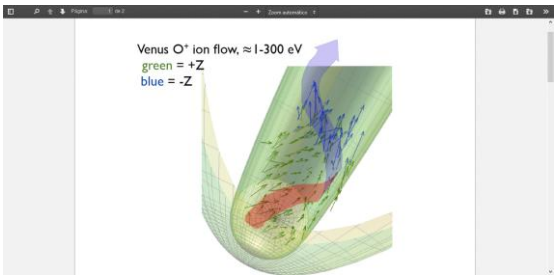

Figure 2. Schematic view of the corkscrew shape in the distribution of velocity vectors of O+ ions inferred from VEX measurements as they move downstream from Venus.

References:

[1] Lundin R., et al., GRL, 116, 40(7), 273, 2013.
[2] Pérez-de-Tejada, H.,INTECH, ISBN 978-953-51-2943-1, 2017.
[3] Drummond, J. E., Plasma Physics, p. 197, McGrawHill,1961.
[4] Pérez-de-Tejada, H. Ap.Jl, 525, L65-68,1 999.

EPSC Abstracts
Vol. 12, EPSC2018-45, 2018
European Planetary Science Congress 2018

Ion Escape from Mars - Observations by Mars Express and MAVEN

Markus Fränz (1), Eduard Dubinin (1), Lukas Maes (1), Jim McFadden (2) and Bruce Jakosky (3)
(1) MPI for Solar System Research, Göttingen, Germany (fraenz@mps.mpg.de),
(2) Space Science Lab.,University of California, Berkeley, CA, USA,
(3) Laboratory for Atmospheric and Space Physics, Univ. of Colorado, Boulder, CO, USA

Abstract

Measuring the escape of ions from Mars has been one of the main targets of the ASPERA-3 experiment on Mars Express since orbit insertion in 2004. But the Mars Express spacecraft is not optimized for this measurement since it lacks a magnetometer and a Langmuir probe to observe magnetic field and total plasma densities. Nevertheless over the last 12 years several studies have been published attempting to determine the total escape flux and its variation with external parameters from ASPERA-3 observations [1, 2, 3]. Especially the contribution of the *cold ions* with energies of less than 5eV to the escape flux has been debated because it is most difficult to measure. Since October 2014 the MAVEN spacecraft is in orbit around Mars with a much larger instrumental suite optimized for measuring the ion outflow. In this paper we reassess observations made by the MEX ASPERA-3 and MARSIS experiments in the light of the MAVEN observations of tailside ion outflow observed between 2014 and 2017. We investigate the influence of the spacecraft potential on the derived flux values and compare ion density observations by the different MAVEN instruments.

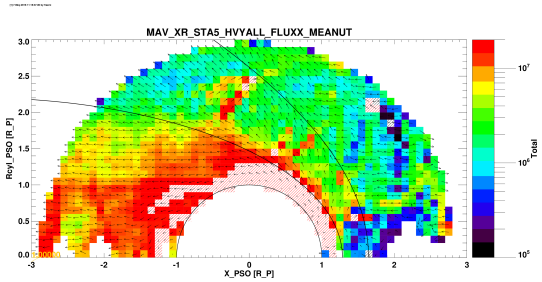

Figure 1: Mean flux of heavy ions (O+ & O2+) observed by MAVEN STATIC between 01 Dec 2014 and 15 Aug 2017, scaled in ions/cm2s. The vertical component of vectors shows the deviation from the cylindrical symmetry axis.

References

[1] Fraenz, M. et al. Plan.Space Science, 119, p.92-104, 2015

[2] Ramstad, R. et al. J.Geophys.Res, 10.1002/2017/JA024306, 2017

[3] Dubinin et al., J.Geophys.Res., 10.1002/2017JA024741, 2017

EPSC Abstracts
Vol. 12, EPSC2018-85, 2018
European Planetary Science Congress 2018

Variability of the martian upper ionosphere and ion escape

Eduard Dubinin (1), Markus Fraenz (1), Martin Pätzold (2), Leila Andersson (3), Jim McFadden (4), Jasper Halekas (5), Jack Connerney (6), Frank Eparvier (3), Paul Mahaffy (6), Oleg Vaisberg (7) and Lev Zelenyi (7)
(1) Max-Planck-Institute for Solar System Research, Goettingen, Germany (dubinin@mps.mpg.de), (2) Rhenish Institute for Environmental Research, Cologne, Germany, (3) Laboratory for Atmospheric, and Space Physics, University of Colorado, Boulder, USA, (4) University of California, Berkeley, USA, (5) University of Iowa, Iowa, USA, (6) NASA Goddard Space Flight Center, USA, (7) Space Research Institute, Moscow, Russia

Abstract

At altitudes above ~200 km, the Martian ionosphere is no longer in photo-chemical equilibrium and strongly variable and complex. We will discuss how different external and internal factors control its variability. We present the observations in the upper ionosphere of Mars carried out by Mars Express and MAVEN spacecraft demonstrating a coupling of the ionosphere with the processes above and below it. Solar EUV flux remains to be important in the upper ionosphere. With increase of the solar irradiance the ionosphere expands above the nominal position of the induced magnetosphere and becomes denser. Solar wind also affects its structure. For example, with increase of the solar wind strength the upper ionospheric layers are density depleted. The upper ionosphere is sensitive to the IMF direction. In the hemisphere, in which the motional electric field is directed toward the planet, the ionosphere is denser and expands to higher altitudes as compared to the ionosphere in the opposite hemisphere. Crustal magnetic field modifies the ionosphere structure producing a large bulge in the southern hemisphere. All these variabilities significantly affect ion losses at Mars.

Acknowledgements

Authors E.D. and M.P. wish to acknowledge support from DFG by grant PA 525/14-1. Authors E.D. and M.F. wish to acknowledge support from DLR by grant 50QM1302. O.V. and L.Z. wish to acknowledge support from the Russian Science Foundation by grant16-42-01 103. The MAVEN observational data used in the study were obtained from the NASA Planetary Data System (PDS).

EPSC Abstracts
Vol. 12, EPSC2018-97, 2018
European Planetary Science Congress 2018

Overview of the Ionospheres of Unmagnetized Solar System Bodies

Thomas E. Cravens (1)
(1) Dept. of Physics and Astronomy, University of Kansas, Lawrence, KS, USA, (cravens@ku.edu)

Abstract

The physical and chemical processes operating in all ionospheres are very similar. Ionospheres are formed when solar radiation or precipitating particles from the external environment (e.g., magnetosphere or solar wind) ionize the upper atmospheres of planets, satellites, or other neutral environments. However, very different density structures, chemical compositions, temperatures, and dynamics result due to differences in the heliocentric distance, strength of the intrinsic magnetic field, size of the planet/object, and the underlying atmospheric composition. An important aspect of ionospheric behavior is magnetosphere-ionosphere coupling and/or the interaction with the solar wind or other external plasma. For planets and bodies with weak intrinsic magnetic fields (e.g., Venus, Mars, Titan, and comets), external magnetospheric or solar wind plasma interacts more directly with the ionosphere and upper atmosphere. The composition, dynamics, and energetics are all affected by this interaction. Data on the ionospheres of non-magnetic bodies is available from many missions including Pioneer Venus, Venus Express, MAVEN, Mars Express, Cassini, and Rosetta. A broad review of this topic will be given.

EPSC Abstracts
Vol. 12, EPSC2018-137, 2018
European Planetary Science Congress 2018

MARSIS observations of field-aligned irregularities and ducted radio propagation in the Martian ionosphere

D. J. Andrews (1), H. J. Opgenoorth (1), T. B. Leyser (1), S. Buchert (1), N. J. T. Edberg (1), D. D. Morgan (2), D. A. Gurnett (2), A. J. Kopf (2), K. Fallows (3), P. Withers (3,4).
(1) Swedish Institute for Space Physics, Uppsala, Sweden (david.andrews@irfu.se), (2) Department of Physics & Astronomy, University of Iowa, IA, USA, (3) Center for Space Physics, Boston University, MA, USA, (4) Department of Astronomy, Boston University, MA, USA,

Abstract

Knowledge of Mars's ionosphere has been significantly advanced in recent years by observations from Mars Express (MEX) and lately MAVEN. A topic of particular interest are the interactions between the planet's ionospheric plasma and its highly structured crustal magnetic fields, and how these lead to the redistribution of plasma and affect the propagation of radio waves in the system. In this paper, we elucidate a possible relationship between two anomalous radar signatures previously reported in observations from the MARSIS instrument on MEX. Relatively uncommon observations of localized, extreme increases in the ionospheric peak density in regions of radial (cusp-like) magnetic fields and spread-echo radar signatures are shown to be coincident with ducting of the same radar pulses at higher altitudes on the same field lines. We suggest that these two observations are both caused by a high electric field (perpendicular to $\mathbf{B}$) having distinctly different effects in two altitude regimes. At lower altitudes, where ions are demagnetized and electrons magnetized, and recombination dominantes, a high electric field causes irregularities, plasma turbulence, electron heating, slower recombination and ultimately enhanced plasma densities. However, at higher altitudes, where both ions and electrons are magnetized and atomic oxygen ions cannot recombine directly, the high electric field instead causes frictional heating, a faster production of molecular ions by charge exchange, and so a density decrease. The latter enables ducting of radar pulses on closed field lines, in an analogous fashion to interhemispheric ducting in the Earth's ionosphere.

1. Observations

In Figure 1 we show four MARSIS ionograms obtained on orbit 2359, close to periapsis at similar altitudes and longitudes, though with significant variation in both latitude and solar zenith angle. The format of each is identical, with reflected intensity shown color-coded versus the sounding frequency f and delay time. All four were taken on the dayside, and each shows a clear ionospheric reflection at a delay of ∼1-1.5 ms.

Figure 1a shows a fairly typical ionospheric reflection trace. The ionogram shown in Figure 1b was obtained at slightly lower altitudes and marginally closer to the sub-solar point than that shown in Figure 1a. The ionospheric reflection is markedly different than that observed in Figure 1a, just northward of the location of the spacecraft in Figure 1b. Firstly, the maximum frequency of the ionospheric trace has significantly increased to ∼4.5 MHz ($n_e \approx 2.4 \times 10^5$ cm^{-3}). This indicates a peak plasma density in the ionosphere well above the $\sim 1.3 \times 10^5 \mathrm{cm}^{-3}$ expected at this solar zenith angle according to models of the 'nominal' ionosphere. Here, the ionospheric trace is everywhere more spread out in delay than the sharp nadir reflection shown in Figure 1a, indicating a very non-planar ionosphere. Nielsen et al. [2007], in an analysis of the iongram shown in Figure 1b and other similar features observed on the same orbit, suggested that these greatly enhanced peak densities could be caused by a two-stream (Farley-Buneman) instability acting in the ionosphere.

Figure 1c was obtained shortly after a second such peak density enhancement and delay spreading event. An additional trace is also discernible below the principal nadir reflection, extending still to high frequencies. We suggest that this additional trace is associated with the peak density enhancement, having effectively "detached" from the original feature and moved to higher delays in the intervening soundings, appearing now in this ionogram at delays of ∼1.9-2.4 ms.

The final ionogram shown in Figure 1d depicts one of the so-called 'epsilon' signatures, reported first in

the Martian ionosphere by [*Zhang et al.*(2016)]. In addition to a more-typical ionospheric reflection similar to that seen in Figure 1a, three connected traces are are also visible over much larger delays of ∼3-4.4 ms. [*Zhang et al.*(2016)] suggest that this particular signature is the result of ducted propagation of the MARSIS sounding pulse in a plasma cavity, by analogy to similar signatures noted in Earth-orbiting topside ionospheric sounders.

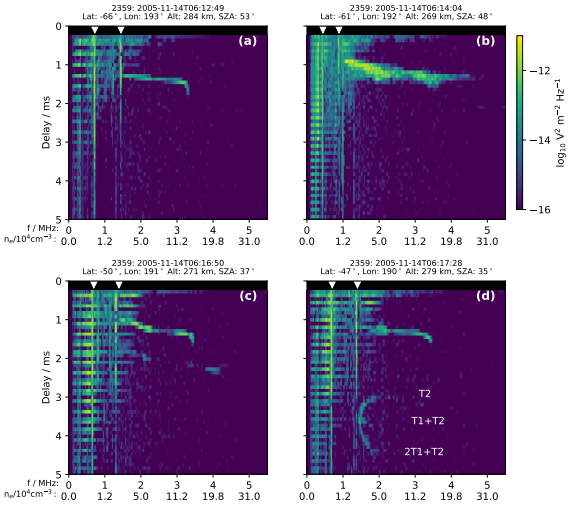

Figure 1: Four MARSIS ionograms obtained on orbit 2359.

2 Interpretation

The two uncommon features noted here – greatly enhanced peak densities and ducted propagation in plasma cavities – are shown to be related to one another. Ionospheric irregularities lying on the same field line are shown to be able to produce both effects, including the delay-spread signatures (Figure 2). Unusually high perpendicular electric fields are shown to be a likely cause of both effects, as the modification of the ionospheric plasma density these will cause will be different at different altitudes. Taken together with other recent observations, this study points towards processes in the Martian ionosphere that share both similarities and significant departures from related processes widely studied in the Earth's ionosphere.

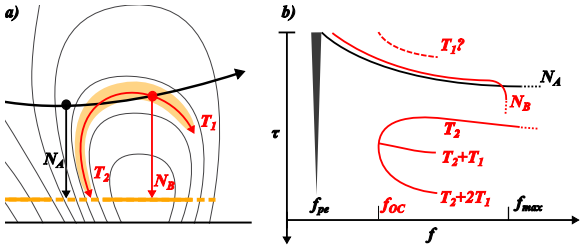

Figure 2: a) MEX's trajectory and MARSIS radar echoes obtained at two locations during a passage through a crustal field arcade, including both nadir and ducted reflections. b) Illustrative features of the two ionograms corresponding to the locations in a), versus time delay τ and sounding frequency f.

Acknowledgements

Work at IRF was supported by grants from the Swedish National Space Agency (DNR 162/14) and the Swedish Research Council (DNR 621-2014-5526). Work at Iowa was supported by NASA through contract 1224107 from the Jet Propulsion Laboratory. Work at Boston University was supported by NASA award NNX15AM59G. All data used in this paper are available in the ESA planetary science archive, https://archives.esac.esa.int/psa.

References

[*Nielsen et al.*(2007)] Nielsen, E., M. Fraenz, H. Zou, J.-S. Wang, D. A. Gurnett, D. L. Kirchner, D. D. Morgan, R. Huff, A. Safaeinili, J. J. Plaut, G. Picardi, J. D. Winningham, R. A. Frahm, and R. Lundin (2007), Local plasma processes and enhanced electron densities in the lower ionosphere in magnetic cusp regions on Mars, *Planet. Space. Sci.*, *55*, 2164–2172, doi:10.1016/j.pss.2007.07.003.

[*Zhang et al.*(2016)] Zhang, Z., R. Orosei, Q. Huang, and J. Zhang (2016), Ducted electromagnetic waves in the Martian ionosphere detected by the Mars Advanced Radar for Subsurface and Ionosphere Sounding radar, *Geophys. Res. Lett.*, *43*, 7381–7388, doi:10.1002/2016GL069591.

EPSC Abstracts
Vol. 12, EPSC2018-230, 2018
European Planetary Science Congress 2018

Correction of Low-Energy Ion Measurements from Rosetta-ICA for the Effects of Spacecraft Charging

Sofia Bergman (1,2), Gabriella Stenberg Wieser (1), Martin Wieser (1) and Fredrik Johansson (3)
(1) Swedish Institute of Space Physics, Kiruna, Sweden (sofia.bergman@irf.se), (2) Umeå University, Sweden,
(3) Swedish Institute of Space Physics, Uppsala, Sweden

Abstract

One common and unwanted effect of spacecraft charging is the interference with scientific measurements. The Ion Composition Analyzer (ICA) onboard the Rosetta spacecraft is designed to make in situ measurements of positive ions in the environment of comet 67P/Churyumov-Gerasimenko. The spacecraft is often charged to a substantial negative potential, which is problematic for the measurements. The ions are attracted to the spacecraft, which for low-energy ions results not only in a change of energy, but also direction of travel. This study aims at determining the influence of the spacecraft potential on the low-energy ion measurements performed by ICA, with the ultimate goal of reconstructing the original ion energies and directions of travel.

1. Introduction

In 2004 the Rosetta spacecraft was launched to study the comet 67P/Churyumov-Gerasimenko. It arrived at the target in 2014 and the mission ended in September 2016 by a controlled impact. Onboard the spacecraft the Rosetta Plasma Consortium (RPC) is a group of instruments designed to study the plasma environment around the comet [2]. One of these instruments is the Ion Composition Analyzer (ICA), an ion spectrometer designed to study the interaction between the solar wind and the cometary particles. Problematic for the measurements is, however, the charging of the spacecraft. A spacecraft in space will interact with the surrounding plasma and acquire an electrostatic potential [1]. In the case of Rosetta the spacecraft was almost exclusively charged to a negative potential throughout the mission. ICA is able to measure ions down to a few eV, but the ions with the lowest energies are heavily affected by the charged spacecraft. This results in a change in both energy and direction of travel. The purpose of this study is to investigate what influence the spacecraft potential has had on the low-energy ion measurements performed by ICA in order to be able to correct the measurements for this effect.

2. Method

The tool used for this study is the Spacecraft Plasma Interaction Software (SPIS). This software can be used to simulate and model the interactions between the spacecraft and the plasma [3]. In SPIS the plasma environment around the spacecraft is simulated from which the plasma potential is obtained. An example of a simulation output is shown in Figure 1. SPIS also offers the possibility to define a scientific instrument to perform advanced calculations, e.g. particle tracing. We use SPIS to implement backward tracing of particles from a particle instrument to analyze the expected deviations in travel direction for different energies.

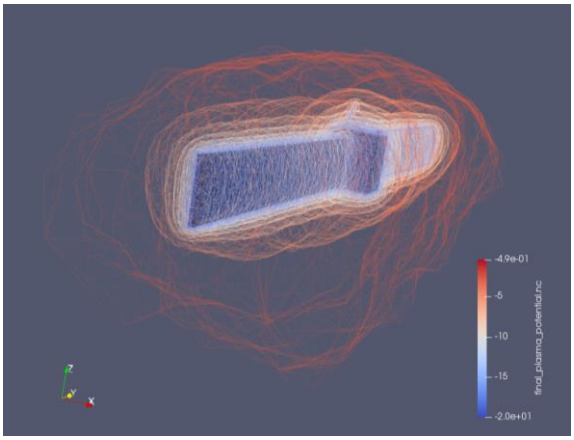

Figure 1: Simulated potential surfaces around the spacecraft. The spacecraft potential was for this simulation set to a fixed value of -20 V, the ion (H_2O^+) and electron densities were set to 1000 cm^{-3}, and the ion and electron temperatures were set to 0.5 and 10 eV respectively. The drift velocity of the ions was set to 4 km/s in the –z direction.

3. First Results

Figure 2 shows simulated selected ion trajectories close to the Rosetta spacecraft. The figure shows that the ion trajectories are clearly affected by the spacecraft. In this case the ions are entering the simulation volume from the –z direction with an initial velocity of 4 km/s (corresponding to an energy of approximately 1.5 eV). They are then accelerated in the potential field around the spacecraft.

The ion spectrometer ICA has a field of view (FOV) of 360°×90°. In the azimuthal direction (360°, corresponding to rotation in the x-z plane in Figure 3) this FOV is divided into 16 segments referred to as sectors, each with a FOV of 22.5° each. This is also the nominal resolution of the instrument in this direction.

By back tracing ions hitting ICA we find their original energy and direction of travel. Figure 3 shows an example where we have back traced ions detected by one of the 16 azimuthal sectors of the instrument. From Figure 3 it is clear that the nominal FOV is distorted for low energies, and the original travel direction of the ions can differ significantly from the travel direction at detection.

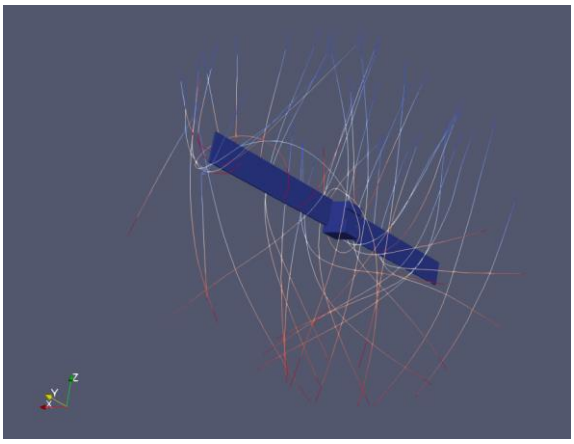

Figure 2: Simulation result from SPIS showing the influence of the spacecraft potential on low-energy H_2O^+ ion trajectories. For further details about the simulation, see Figure 1.

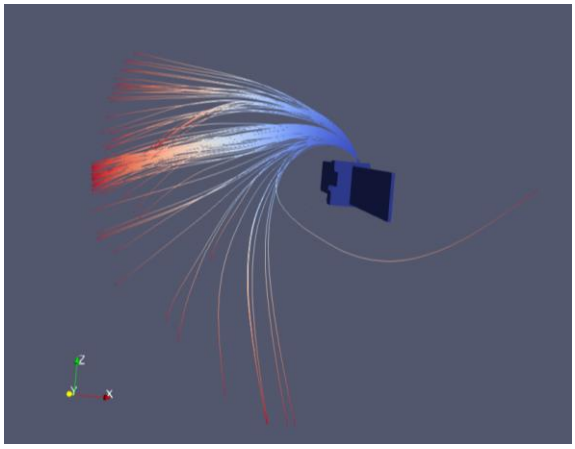

Figure 3: Simulation result from SPIS where low-energy H_2O^+ ions are traced backwards from one of the sectors of the instrument. At the edge of the simulation volume these ions have an energy of approximately 2 eV. For further details about the simulation, see Figure 1.

4. Expected Results

The first results of the study will be presented, including an analysis of the deviation in travel direction for the ions at different energies for each sector of the instrument. We expect the distortion to be more severe for lower energies, and we expect to be able to find an energy threshold above which it is possible to correct the data to reconstruct the original direction and energy of the ions.

References

[1] Garrett, H. B.: The Charging of Spacecraft Surfaces, Reviews of Geophysics and Space Physics, Vol. 19, No. 4, pp. 577-616, 1981.

[2] Nilsson, H., Lundin, R., Lundin, K., Barabash, S., Borg, H., Norberg, O., Fedorov, A., Sauvaud, J.-A., Koskinen, H., Kallio, E., Riihelä, P. and Burch, J. L.: RPC-ICA: The Ion Composition Analyzer of the Rosetta Plasma Consortium, Space Science Reviews, Vol. 128, pp. 671-695, 2007.

[3] Thiébault, B., Mateo-Velez, J.-C., Forest, J. and Sarrailh, P.: SPIS 5.1 User Manual, Version 3, Revision 4, 2013.

EPSC Abstracts
Vol. 12, EPSC2018-250, 2018
European Planetary Science Congress 2018

The effect of solar flares on comet 67P and RPC/LAP

Niklas J.T. Edberg (1), Fredrik L. Johansson (1), Anders. I. Eriksson (1), Cyril Simon Wedlund (2), Markku Alho (3), David J. Andrews (1), Elias Odelstad (1), Erik Vigren (1) and Pierre Henri (4)
(1) Swedish Institute of Space Physics, Uppsala, Sweden (ne@irfu.se), (2) Department of Physics, University of Oslo, Norway, (3) Department of Radio Science and Engineering, School of Electrical Engineering, Aalto University, Aalto, Finland, (4) Laboratoire de Physique et Chimie de l'Environnement et de l'Espace (LPC2E), CNRS, Orleans, France

Abstract

We investigate the effects of solar flares on the coma of comet 67P as well as their influence on the photoelectron current from the RPC/LAP instrument. During the ~2 years Rosetta spent in the vicinity of comet 67P, ~4500 solar flares were observed to occur on the Sun, through X-ray flux measurements by the GOES satellite in orbit around Earth. 1600 of those occurred on regions on the Sun viewable from the vantage point of Rosetta, of all classes (A, B, C, M, X). We find that only a minority of the events have any noticeable effects on the measured photoelectron current by the Langmuir probe (LAP). We find little evidence of the flares having any effect on the cometary coma in terms of increased electron density. However, observing this is complicated due to the otherwise dynamic plasma environment in combination with measurement uncertainties. The effect on the plasma density is still under investigation. Only a few large solar flare events (X-class) were reported, whose intensity might be needed to cause any significant effects.

EPSC Abstracts
Vol. 12, EPSC2018-274, 2018
European Planetary Science Congress 2018

Cometary plasma response to interplanetary corotating interaction regions during 2016 June – September: a quantitative study by the Rosetta Plasma Consortium

Rajkumar Hajra (1), Pierre Henri (1), Minna Myllys (1), Kevin L. Heritier (2), Marina Galand (2), Cyril Simon Wedlund (3), Hugo Breuillard (1,4), Etienne Behar (5), Niklas J. T. Edberg (6), Charlotte Goetz (7), Hans Nilsson (5), Anders I. Eriksson (6), Raymond Goldstein (8), Bruce T. Tsurutani (9), Jerome More (1), Xavier Vallieres (1), Gaetan Wattieaux (10)

(1) LPC2E - CNRS, Orleans, France (rajkumarhajra@yahoo.co.in), (2) Department of Physics, Imperial College London, Prince Consort Road, London, SW7 2AZ, UK, (3) Department of Physics, University of Oslo, Box 1048 Blindern, 0316 Oslo, Norway, (4) Laboratoire de Physique des Plasmas, Ecole Polytechnique/CNRS/Sorbonne Universit´e, 4 Place Jussieu, Paris, France, (5) Swedish Institute of Space Physics, P.O. Box 812, 981 28 Kiruna, Sweden, (6) Institutet for rymdfysik, Angstrom Laboratory, Lagerhyddsvagen 1, Uppsala, Sweden, (7) Institut fur Geophysik und extraterrestrische Physik, TU Braunschweig, Mendelssohnstr. 3, 38106 Braunschweig, Germany, (8) Southwest Research Institute, PO Drawer 28510, San Antonio, TX 78228-0510, USA, (9) Jet Propulsion Laboratory, California Institute of Technology, 4800 Oak Grove Drive, Pasadena, CA 91109, USA, (10) LAPLACE, Universite de Toulouse, CNRS, F-31062 Toulouse, France

Abstract

Four interplanetary corotating interaction regions (CIRs) were identified during 2016 June through September by the Rosetta Plasma Consortium (RPC) monitoring in situ the plasma environment of the comet 67P/Churyumov-Gerasimenko (67P) at the heliocentric distances of ~3 and 3.8 au. The CIRs, formed in the interface region between low- and high-speed solar wind streams with speeds of ~320-400 km s^{-1} and ~580-640 km s^{-1} respectively, are characterized by relative increases in solar wind proton density by ~13-29, in proton temperature by ~7-29, and in magnetic field by ~1-4 with respect to the pre-CIR values. The CIR boundaries are well-defined with interplanetary discontinuities. Out of 10 interplanetary discontinuities at the CIR boundaries, 4 are determined to be forward waves and 5 are reverse waves, propagating at ~5-92% of the magnetosonic speed at angles of ~19.8°-86.6° relative to ambient magnetic field. Only one is identified to be a quasi-parallel forward shock with magnetosonic Mach number of 1.48 and shock normal angle of 41.0°. The response of the cometary ionosphere was monitored by Rosetta from cometocentric distances of ~4 to 30 km. A quiet time plasma density map was developed by considering the effects of varying cometary latitude, longitude and cometocentric distance of the Rosetta observations before and after each of the CIR intervals. The CIRs lead to plasma density enhancements of ~500-1000% with respect to the quiet time reference level. Ionospheric modeling shows that increased ionization rate due to enhanced ionizing suprathermal (>12-200 eV) electron impact is the prime cause of the large cometary plasma density enhancements during the CIRs. Plausible origin mechanisms of the cometary suprathermal electron enhancements are discussed.

EPSC Abstracts
Vol. 12, EPSC2018-319-1, 2018
European Planetary Science Congress 2018

Variability of the precipitating fluxes during September 2017 event

Martinez Antoine [1], Leblanc F. [1], Witasse O.[2], Modolo R.[3], Titov D.[2], Chaufray J.Y.[3], Romanelli N.[3] and MAVEN team

[1]LATMOS/IPSL, Sorbonne Université, CNRS, Paris, France, [2] ESA/ESTEC, The Netherlands, [3]LATMOS/IPSL, UVSQ Université Paris-Saclay, CNRS, Guyancourt, France

Abstract

We here study the influence of several solar atmospheric and magnetospheric forcing drivers, during September 2017 solar event. We focus on the fluxes of precipitating heavy ion towards Mars' atmosphere as seen by MAVEN: SWIA (cs product), an energy and angular ion spectrometer and by STATIC (d1 and c6 products), an energy, mass and angular ion spectrometer. [1]

1. Introduction

Although atmospheric sputtering is a minor component of atmospheric escape today, it is thought to have been much more important four billion years ago [2]. Heavy ion precipitating is the primary driver of atmospheric sputtering. September 2017 solar event provides a unique opportunity to study the role of several solar potential drivers of heavy ion precipitation. In this presentation, we will present how the precipitating flux changed all along September 2017 solar event and will discuss what can be derived on the dependency of this precipitation with respect to our Sun.

1.1 Background trouble

During September 2017 event, Solar Energetic Particles (SEPs) induce a strong background on SWIA measurements. In the case of STATIC, its technic of measurements allows it to significantly reduce the impact of SEP event on its measurements. We therefore develop a numerical treatment to subtract it to SWIA.

2. Methodology of background value reconstruction

The background is characterized by a flat energy spectrum of the energy differential flux (in eV/cm^2/s/eV/str). We therefore used this characteristic in order to estimate it. For instance, we observed on the 12th September a background value around 3×10^5, instead of 6×10^3 during nominal period. To correct SWIA data, we therefore perform the following steps:

1 – Calculation of the flux measured by each anode of SWIA on 10 min intervals (144 intervals per day). The background is reconstructed from the highest energy range of SWIA (>5 keV) if the energy flux is constant within this range.
2 – The set of reconstructed backgrounds 40 min before and after is then used to estimate the background within 200 and 350 km in altitude.
3 – We then subtract the value of this background to SWIA.

3. Maven Measurements

There are five periods in September 2017, as represented on the figure 1, during which the precipitating flux exceeds by more than 3 sigma the average value measured during the 30-31 August and 25-26 September (considered as reference periods for nominal solar conditions). During this period, MAVEN's periapsis drifts slowly in longitude/latitude. However, when reconstructing the precipitating flux (between 200 and 350 km in altitude), we only considered the inbound portion of the orbits to further limit the range of SZA and latitude/longitude covered by MAVEN during September 2017.

In order to explain this variability, we have to consider the main potential solar drivers for the precipitating flux which are:

- the EUV flux,
- the SEPs flux,
- the solar wind parameters which can be partially represented by the electric field of convection. Here, we used the |VxB| as measured at MAVEN apoapsis.

Another driver is the solar wind dynamic pressure which is however difficult to reconstruct without direct solar wind measurements. The increase of the dynamic pressure between late 12th to 14th September compressed Mars' magnetosphere and favored the acceleration and precipitation of the planetary picked-up ions. [3]. As a consequence, a sharp increase in precipitating flux could be seen in STATIC measurements at low energy and in SWIA measurements at high energy. But, we believe that it is probably the combination of the preceding SEPs event, the flare and of the ICME arrival which leads to the maximum of precipitating flux observed during September 2017 event.

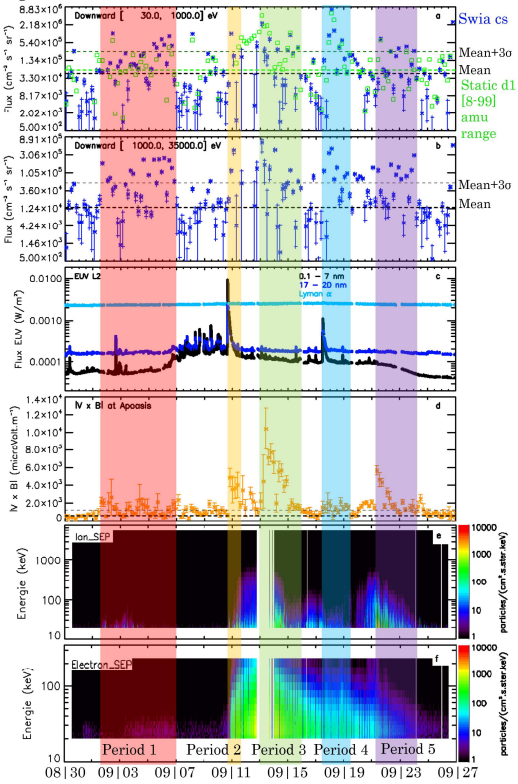

Figure 1: Measured SWIA integrated precipitating flux and few potential drivers for the precipitating flux during September 2017 period. Integrated precipitating flux of September 2017 **(a)** 30 and 1000 eV energy range, **(b)** 1 and 25 keV energy range. Green square: Static d1 8-99 amu mass range. Blue star: Swia cs. The horizontal black (green) thick dashed line corresponds to the average value of SWIA (STATIC D1) precipitating flux during the two periods encompassing September 2017 event. The thin dashed horizontal line corresponds to the average value plus 3 times the standard deviation with respect to this average during these two periods. Errors bars on panels a and b correspond to 1 sigma deviation of the corresponding reconstructed background. **(c)** Value of the EUV photon flux as measured by EUV instrument/MAVEN, blue light line: 121-122 nm band, blue line: 17-22 nm range and black line 0.1-7 nm range. **(d)** Intensity of $\|\vec{V} \times \vec{B}\|$ reconstructed from SWIA moments and MAG measurements at MAVEN apoapsis. **(e)** Ion flux measured by SEP/MAVEN F1 detector within 20 keV and 70 MeV. **(f)** Electron flux measured by SEP/MAVEN F1 detector within 20 keV and 300 keV.

4. Summary and Future work

September 2017 solar event is a unique opportunity to analyze what could be the respective role of the solar drivers inducing intense heavy ion precipitation into Mars' atmosphere.

After a careful reconstruction of the background induced by the SEPs event on SWIA spectrometer, we were able to investigate the precipitating flux responses to the solar energetic event of September 2017. This study shows an increase in precipitation flux of more than one order of magnitude during solar events compared to the average flux of a similar period but for quiet solar.

Acknowledgements

AM acknowledges the support of DIM ACAV and ESA/ESTEC. This work was also supported by CNES "Système Solaire" program and by the Programme National de Planétologie and Programme National Soleil-Terre. This work is also part of HELIOSARES Project supported by the ANR (ANR-09-BLAN-0223) and ANR MARMITE (ANR-13-BS05-0012-02).

References

[1] Leblanc F., R. Modolo and al. (2015), Geophys. Res. Lett, 42, 9135-9141, doi : 10.1002/2015GL066170.

[2] Luhmann, J.G., Johnson, R.E., Zhang, M.H.G., (1992), Geophys. Res. Lett., 19, 21, 2151-2154.

[3] S. M. Curry, J. G. Luhmann, and al. (2015), Geophys. Res. Lett, 42, 9095-9102, doi: 10.1002/2015GL06304.

EPSC Abstracts
Vol. 12, EPSC2018-417, 2018
European Planetary Science Congress 2018

Comparative aeronomy of cometary and planetary ionospheres: solar energy deposition and plasma loss

Arnaud Beth
Department of Physics, Imperial College London, Prince Consort Road, London SW7 2AZ, United Kingdom (abeth@ic.ac.uk)

Abstract

European Space Agency (ESA) missions Giotto and Rosetta offered us the best opportunities to probe the cometary ionospheres of 1P/Halley and 67P/Churyumov-Gerasimenko. During the 2-year Rosetta escort phase, different conditions were encountered at 67P and played a key role in the structure and variability of its ionosphere: strong variation in the outgassing rate and in the ionization frequency by extreme ultraviolet solar radiation, for instance. In particular, Rosetta spotlighted that 67P is very different from 1P.

Cometary environments are atypical of planetary ones. Their gaseous envelopes – comae – are neither gravitationally bounded to the surface nor in hydrostatic equilibrium. Actually, comae result from the sublimation of ices turned into gas which expands into the space vacuum at several hundred metres per second. The lack of gravity leads to an unprecedented and unpredicted feature for cometary ionospheres: the maximum of solar energy deposition does not occur at the same optical depth as what is observed in planetary ionospheres.

During this presentation, I will contrast the structure of cometary ionospheres with planetary ones. First, I will focus on the production of photo-electrons and its altitude profile for both cases. Secondly, I will show how it is impacted by the cometary activity, and how it varies with the heliocentric distance. Finally, I will address the consequences on the electron number density profile. Especially, I will spotlight and cover the relevant processes ongoing in the cometary ionospheres under different conditions encountered at comet 1P during Giotto and comet 67P during the Rosetta escort phase.

EPSC Abstracts
Vol. 12, EPSC2018-437, 2018
European Planetary Science Congress 2018

Study of the couplings in the Mars' atmosphere with the Mars Express MARSIS total electron content data set

Olivier Witasse (1), Beatriz Sánchez–Cano (2), Mark Lester (2), Pierre-Louis Blelly (3), Mikel Indurain (3), Marco Cartacci (4)

(1) European Space Agency, ESTEC – Scientific Support Office, Noordwijk, The Netherlands.
(2) Department of Physics and Astronomy, University of Leicester, United Kingdom.
(3) Institut de Recherche en Astrophysique et Planétologie (IRAP), Toulouse, France.
(4) Istituto Nazionale di Astrofisica (INAF), Istituto di Astrofisica e Planetologia Spaziali (IAPS), Rome, Italy.

Abstract

Ten years of Mars Express Total Electron Content (TEC) data from the Mars Advanced Radar for Subsurface and Ionospheric Sounding (MARSIS) instrument are analysed. We describe the spatial, seasonal, and solar cycle behaviour of the TEC. The TEC temporal profile shows a peak at Ls=25°-75° which is not related to the solar irradiance variation, but instead coincides with an increase in the thermospheric density, possibly linked to lower atmosphere cycles. With the help of numerical modelling, we compute the contribution of the ion species to the TEC, which allows the study of the coupling between the thermosphere and the ionosphere. We show that the TEC is a useful parameter, routinely measured by Mars Express, to investigate the couplings at work in the Mars' atmosphere.

1. Introduction

The Martian atmosphere is a highly variable system in which the lower and upper parts are strongly coupled. The ionosphere and the thermosphere are closely connected, and influenced by several external and internal forcing mechanisms, such as space weather or gravity waves respectively among many others. In this work, we evaluate how the TEC variations are linked to the seasonal variability of the thermosphere. In addition, we assess the latitudinal response of this atmospheric coupling, its solar activity and solar illumination dependences.

2. Ionosphere-Thermosphere simulation

A numerical simulation of the ionosphere of Mars during a Martian year has been performed in order to evaluate the role of the neutral atmosphere in the TEC variation observed in the Mars Express MARSIS dataset. We have used the Mars version of the numerical/physical model IRAP plasmasphere-ionosphere model (IPIM). The IPIM model can be run from the Transplanet's Space Weather Prediction Center (http://transplanet.cdpp.eu). This model uses as inputs the Mars Climate Database (MCD), built from the Global Circulation Model (GCM) developed at Laboratoire de Meteorologie Dynamique (LMD). The model was run for a fixed solar flux in order to avoid TEC variability due to solar irradiance/solar activity, and to assess the role that the neutral atmosphere has on the ionosphere as a function of season and latitude. Model outputs reproduce the changes in the TEC temporal profile, and seem to confirm the atmospheric coupling. The simulation also allows us to identify the neutral and ionized species that play a role in the thermosphere and ionosphere during each season.

Conclusions

In this work, we show that the TEC observations routinely made by Mars Express-MARSIS can be used to monitor the behaviour of the Martian atmosphere.

Acknowledgements

B.S.-C. and M.L. acknowledge support through STFC grant ST/N000749/1. ESA-ESTEC Faculty is also gratefully acknowledged.

EPSC Abstracts
Vol. 12, EPSC2018-444, 2018
European Planetary Science Congress 2018

Indirect identification of a low-altitude layer in the Martian nightside ionosphere during a space weather event with Mars Express-MARSIS radar data

Beatriz Sanchez-Cano (1), Mark Lester (1), Olivier Witasse (2), Marco Cartacci (3), Pierre-Louis Blelly (4), Hermann Opgenoorth (5), François Leblanc (6), Rob Lillis (7), Nicolas Floury (2)

(1) Department of Physics and Astronomy, University of Leicester, Leicester, UK (bscmdr1@leicester.ac.uk)
(2) European Space Agency, ESTEC, Noordwijk, The Netherlands
(3) Istituto Nazionale di Astrofisica (INAF), Istituto di Astrofisica e Planetologia Spaziali (IAPS), Rome, Italy
(4) Institut de Recherche en Astrophysique et Planétologie (IRAP), Toulouse, France
(5) Swedish Institute of Space Physics, Uppsala Division, Uppsala, Sweden
(6) LATMOS/IPSL, CNRS, Sorbonne Université, UVSQ, Paris, France
(7) Space Sciences Laboratory, University of California, Berkeley, California, USA

Abstract

The Mars Advanced Radar for Subsurface and Ionosphere Sounding (MARSIS) on board the Mars Express (MEX) mission suffered from a complete blackout for 10 days in September 2017 when it was sampling the subsurface of the planet during the nightside. We propose that this blackout of MARSIS data was caused by the solar energetic particles (SEP) of few tens of keV associated with a space weather event that hit Mars between the ~11th and the 21st of that month. Electron precipitation are believed to produce a low ionospheric layer on the nightside, which absorbed the radar signals. In this study, we assess the properties of this low ionospheric layer based on the radar attenuation observations.

1. Introduction

September 2017 was a very active month in terms of space weather. The Sun emitted the two largest solar flares of the current solar cycle, a X9.3 flare on the 6th and a X8.2 flare on the 10th. This second flare was accompanied by a large coronal mass ejection (CME) that arrives at Mars on the 13th, and by a solar energetic particle (SEP) event that hit Mars during 10 days starting few minutes after the flare was emitted on the 10th of September.

All spacecraft at Mars detected this space weather event. At that time, the MARSIS radar aboard Mars Express was sampling the southern hemisphere subsurface on the nightside and suffered from a complete blackout for 10 days (Figure 1).

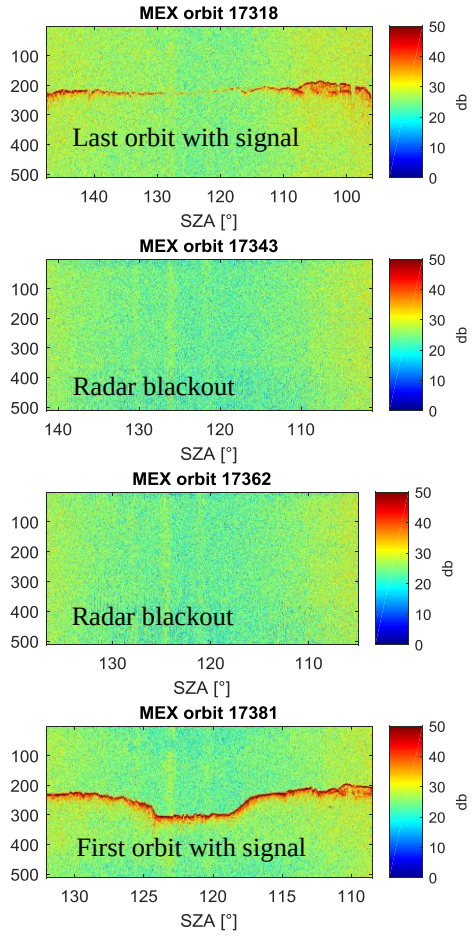

Figure 1: Example of MARSIS data with and without radar blackout during this space weather event

The timing of this blackout coincides well with the observations of the electrons from the SEP event duration measured by the MAVEN spacecraft.

In this study, we interpret the radar blackout as the effect caused by the absorption of a low ionospheric layer formed from precipitation of SEP electrons.

2. Radar signal attenuation

It is well established at Earth that energetic electron and proton precipitation can produce enhancements of the lower ionospheric layers, the D and E layers, which then absorb radio signals. At Mars, previous studies have shown that different phenomena, such as meteoritic showers, CMEs, corotating interaction regions (CIRs) or SEPs, can result in radar absorption both on the nightside and dayside due to a rise in the electron density of the low ionosphere [1, 2, 3, 4, 5]. However, no spacecraft has ever directly measured this low ionospheric layers, and it is not clear which is the source of ionization that is able to produce a continue 10-day radar blackout on the deep nightside of Mars.

In this study, we start from the level of attenuation that the MARSIS radar signal suffered, and after considering the radar frequencies, the appropriate electron-neutral collision frequency of the nightside atmosphere, and the altitude deposition of the SEP particles, we indirectly estimate the properties and possible shape of the ionospheric absorption layer created by this space weather event.

3. Summary and Conclusions

In this work, we assess the shape and main properties of the ionospheric layer formed at low altitude on the nightside ionosphere after the impact of a powerful space weather event at Mars. We also discuss the most probably source of continuous ionization that led to this low ionospheric layer to survive for 10 days. This work will lead to an improved assessment of radar performances during space weather events.

Acknowledgements

B.S.-C. and M.L. acknowledge support through STFC grant ST/N000749/1. ESA-ESTEC Faculty is also gratefully acknowledged.

References

[1] Witasse, O., J. F. Nouvel, J. P. Lebreton, and W. Kofman (2001), HF radio wave attenuation due to a meteoric layer in the atmosphere of Mars, Geophys. Res. Lett., 28(15), 3039–3042.

[2] Morgan, D. D., et al. (2010), Radar absorption due to a corotating interaction region encounter, Icarus, 206, 95–103.

[3] Espley, J. R., W. H. Farrell, D. A. Brain, D. D. Morgan, B. Cantor, J. J. Plaut, M. H. Acuña, and G. Picardi (2007), Absorption of MARSIS radar signals: Solar energetic particles and the daytime ionosphere, J. Geophys. Res., 34, L09101, doi:10.1029/2006GL028829.

[4] Nemec, F., D. D. Morgan, C. Diéval, and D. A. Gurnett (2015), Intensity of nightside MARSIS AIS surface reflections and implications for low-altitude ionospheric densities, J. Geophys. Res. Space Physics, 120, doi:10.1002/2014JA020888.

[5] Withers, P. (2011), Attenuation of radio signals by the ionosphere of Mars: Theoretical development and application to MARSIS observations, Radio Sci., 46, RS2004, doi:10.1029/2010RS004450.

EPSC Abstracts
Vol. 12, EPSC2018-521, 2018
European Planetary Science Congress 2018

Observations with MEX and MAVEN in the Martian tail during late 2016

Katerina Stergiopoulou, David Andrews
Swedish Institute of Space Physics, Uppsala, Sweden
(katerina.stergiopoulou@irfu.se, david.andrews@irfu.se)

Abstract

We investigate electron density variations in the Martian tail using Mars Express (MEX) measurements from September 2016. MARSIS (Mars Advanced Radar for Subsurface and Ionosphere Sounding), operated in Active Ionospheric Sounding (AIS) mode can determine the local plasma density, as the sounder excites oscillations at the plasma frequency and its higher harmonics. Here, we present data from five non-consecutive MEX orbits, namely 16130, 16133, 16136, 16144 and 16148. These derived electron density time series, when combined with MAVEN LPW, SWIA and MAG measurements for the same time period as the MEX orbits draw a more detailed picture of the correlation between Solar Wind activity and day-to-night transport processes. We show that the electron density well above the ionospheric peak is highly variable with three of the orbits (16130, 16133, 16148) having periods of zero electron density when MEX was located in the shadow, while in two of the orbits (16136, 16144) plasma density structures are present even for solar zenith angles as large as 180 degrees. We study also the crustal magnetic fields as an additional factor that affects the flow and behaviour of nightside ionospheric plasma.

1. Observations

The MARSIS instrument is a low frequency radar on board MEX, which measures the time delay of a transmitted pulse, that can not further propagate below the electron plasma frequency, as a function of the transmitted frequency[1]. The determination of the altitude of the ionospheric peak is feasible when MARSIS operates in AIS mode for altitudes below 1200 km[1]. However, during the orbits presented, MARSIS was operated at altitudes higher than 3000 km which gives us an insight about the local electron density in the deep magnetotail.

In Fig. 1, timeseries of the frequency for each one of the orbits of interest as well as the spatial evolution of MEX are presented. Time is plotted with respect to the periapsis passing and the duration for each orbit is $\sim 50\mathrm{min}$. The local plasma frequency can be distinguished at low frequencies, whereas the harmonics are observed at slightly higher frequencies.

2. Figures

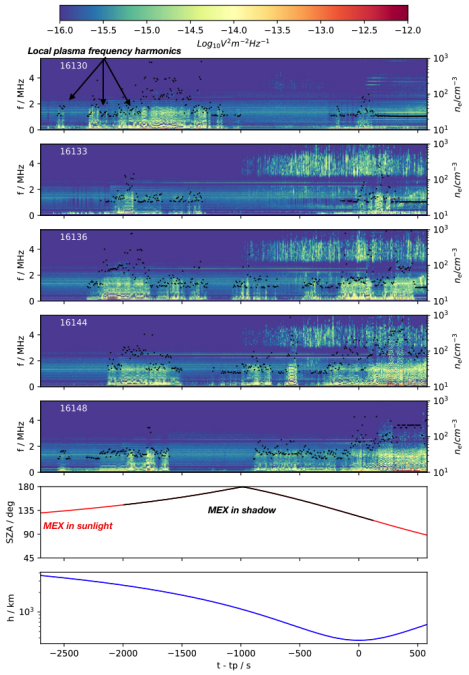

Figure 1: Timeseries of the five orbits of interest.

3. Conclusions

MEX and MAVEN measurements combined allow us to perform a thorough study of the plasma transport processes through the Martian terminator and to the nightside. Moreover, evidence of interaction between the solar wind, the crustal magnetic fields and the observable small scale plasma structures is apparent through the analysis of both MEX and MAVEN data. These observations of the upper ionosphere confirm a variability in the nightside plasma and point out the need for further investigation.

Acknowledgements

This work was supported by a grant from the Swedish National Space Agency, DNR 156/16.

References

[1] Gurnett D. A. et al., Science, 310, 5756 (2005).

EPSC Abstracts
Vol. 12, EPSC2018-605, 2018
European Planetary Science Congress 2018

The Martian Ionosphere's Response to Solar drivers

Laila Andersson (1), C.M. Fowler(1), M. Fillingam2, J. Halekas(3), J. Espley(4), E. Thiemann(1) , D. Mitchell (3), J. McFadden (2), M. K. Elrod (4), and G. A. DiBraccio (4).
(1) LASP, University of Colorado, USA, (2) SSL, University of California, USA, (3) University of Iowa, USA, (4) NASA GSFC, USA. (laila.andersson@lasp.colorado.edu)

Abstract

A six week time period of NASA Mars Atmosphere and Volatile EvolutioN (MAVEN) mission data have be analyzed to gain a greater understanding of the conditions under which the Sun can most effectively drive observable changes in the Martian ionosphere. Seven different types of solar events were analyzed in detail, and were ascribed the following names: magnetic reconnection, pressure pules, solar flare, ICME, low solar wind density, magnetosonic waves, and FAC associated with Martian crustal fields. These events were evaluated based how effectively the conditions in the lower ionosphere changed. One interesting observation was that for the pressure pulse case the lower ionosphere was shielded off, resulting in an almost unperturbed lower ionosphere. The reconnection and the FAC events can drive observable changes but due to their nature they are localized and short lived temporally, decreasing their importance. Based on these events, the magnetosonic waves case was the most effective at modifying the lower ionosphere and lead to significant atmospheric loss.

1. Introduction

The physical processes that drive atmospheric loss at Mars both now and in the past are not fully understood. The main purpose of the MAVEN mission is to study the current day active atmospheric loss processes at Mars and to evaluate which processes could be dominant in the planet's past [1]. The MAVEN mission has demonstrated that neutral atomic oxygen is the dominant loss path for Mars today. But in the past the dominant oxygen loss may have been through ion loss [2].

Therefore, it is important to understand what processes/solar events drive the largest oxygen ion loss at present day Mars. Up to now the focus has mainly been on solar EUV irradiance levels and the solar wind pressure.

The presented study has identified a time period where many different types of solar events are observed, and has evaluated how important each event was in driving observable changes in the lower (<~300 km) Martian ionosphere. Since the study was conducted over a limited time period the ionospheric measurements are made in the same region and under similar EUV conditions, allowing the events to be inter-compared. If a longer time period were to be used then the large ionospheric variability with respect to local time would need to be taken into consideration, resulting in a much more difficult data set to evaluate.

2. The Events

The data are taken from the August – September 2017 time period where the events were selected based on the in-situ measured EUV intensity, and plasma conditions in the upstream sheath region. Six different type of events were identified, as shown in Figure 1, and labeled magnetic reconnection event, pressure pulse, solar flare, ICME, low solar wind density, magnetosonic waves, and FAC associated with crustal fields.

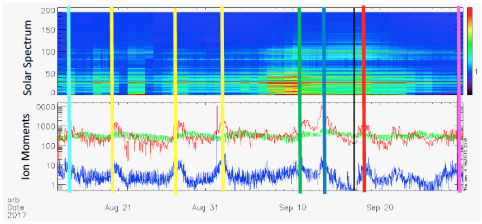

Figure 1: The normalized EUV intensity (top panel) and solar wind (bottom panel) information of the time period of interest. The vertical lines are: reconnection (no 1), pressure pules (no 2,3 and 4), solar flare (no 5), ICME (no 6), low density (no 7), magnetosonic waves (no 8) and FAC (no 9).

The spacecraft orbit was such that inbound segments of periapsis were over the dusk terminator, while the outbound segments were over north pole. The orbit

geometry allowed the plasma to be evaluated as terminator transport, and the magnetic field orientation could be used to infer the draped magnetic field configuration.

3. Ionospheric Shielding

For the three pressure pulse the orbit configuration provided evidence that the lower ionosphere can be magnetically shielded from the upper ionosphere. This resulted in the upper ionosphere, where oxygen densities are relatively low, being significantly modified, but no obvious effects were observed in the lower ionosphere where oxygen densities are much larger.

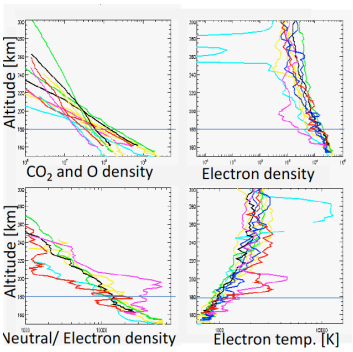

Figure 2: Altitude profiles for the different events identified in Figure 1.

For the ICME event the same was inferred, but not definitely observed. The lower ionosphere was not significantly affected, however, the energy content of the ICME, and variability of the solar wind, were much greater than for the pressure pulse, and this shielding is thus inferred.

4. Most Effective Event

The event most effective at driving changes in the lower ionosphere was that identified as magnetosonic waves. In Figure 2 the neutral and plasma conditions are presented color coded based on the vertical lines in Figure 1.

The magnetosonic wave event is shown by the pink line indicating an over-dense ionosphere with respect to the neutral atmosphere and is associated with enhanced electron temperatures. As has been shown, magnetosonic waves can heat the plasma [3], and with the observed plasma transport here these waves are the most effective way to drive ions from the lower Martian ionosphere, for the events studied here.

The FAC event is shown as the red line and is an outlier. The event is driven by pressure in the solar wind. The observed profiles indicate an under-dense ionosphere with respect to the neutral atmosphere and as a result enhanced electron temperatures are present to refill the flux tube. Since the FAC event is localized in space and temporally short, one can expect that the effect is minor. The reconnection event which occurred on the outbound pass impacted the ionosphere on a short timescale over a localized region only.

5. Summary and Conclusions

Using MAVEN data, the effectiveness of solar events at driving changes in the lower ionosphere are contrasted against each other. Contrary what is expected, an enhanced pressure pulse in the solar wind did not increase the ion outflow from the lower ionosphere. The most effective way, as identified, was the presence of magnetosonic waves that heat the lower ionosphere and drive significant ion loss. Therefore, the occurrence and duration of such wave heating events should be evaluated over Mars' history when considering atmospheric loss over time.

Acknowledgements

This work was supported by contract funds from the NASA MAVEN mission.

References

[1] Jakosky, B.M. et al. Space Sci Rev (2015) 195: 3. https://doi.org/10.1007/s11214-015-0139-x.

[2] Ergun, R.E., et al. (2016), Enhanced O2+ loss at Mars due to an ambipolar electric field from electron heating, J. Geophys. Res. Space Physics, 121, 4668–4678, doi:10.1002/2016JA022349.

[3] Fowler C.M. et al. (2018) MAVEN observations of solar wind driven magnetosonic waves heating the Martian dayside ionosphere, J. Geophys. Res. Space Physics accepted 2018JA025208R.

EPSC Abstracts
Vol. 12, EPSC2018-613-1, 2018
European Planetary Science Congress 2018

Reduced Atmospheric Ion Escape Above Martian Crustal Magnetic Field

Kai Fan[1, 2], Yong Wei[1, 2], Markus Fraenz[3], Eduard Dubinin[3], Jun Cui[4, 5], Qianqian Han[1, 2], Lihui Chai[1], Zhaojin Rong[1], Jun Zhong[1], Weixing Wan[1], J. Mcfadden[6], J. E. P. Connerney[7]

[1]Key Laboratory of Earth and Planetary Physics, Institute of Geology and Geophysics, Chinese Academy of Sciences, Beijing, China.

[2]College of Earth and Planetary Sciences, University of Chinese Academy of Sciences, Beijing, China.

[3]Max-Planck-Institute for Solar System Research, Goettingen, Germany.

[4]Key Laboratory of Lunar and Deep Space Exploration, National Astronomical Observatories, Chinese Academy of Sciences, Beijing, China.

[5]Sun Yat-Sen University, School of Atmospheric Sciences, Zhuhai, China.

[6]University of California, Space Sciences Laboratory, 7 Gauss Way, Berkeley, CA, USA.

[7]NASA, Goddard Space Flight Center, Planetary Magnetospheres Laboratory, Solar System Exploration Division, Greenbelt, MD, USA.

Corresponding author: Yong Wei (weiy@mail.iggcas.ac.cn)

Abstract

Evolution of atmosphere is tightly related to planetary habitability, during the history of solar system. Disappearing of liquid water on Mars and Venus is frequently understood as a consequence of enhanced atmospheric escape, when their magnetic dynamo ceased billions of years ago, as comparing to present Earth with active dynamo and deep oceans. However, such a hypothesis that planetary dipole magnetic field protects its atmosphere from Solar wind's erosion does not have enough supporting evidence, but has been questioned recently. The fast-changing solar wind conditions and the varieties between different terrestrial planets made comparison between dipole magnetic and non-magnetic bodies hard to clarify magnetic field's effect alone. Mars is a natural laboratory since its partially distributed Crustal field on its southern hemisphere and a lack of Earth-like global magnetic field. Locally distributed Crustal field provide a hemisphere possessed magnetic environment which gives The Mars Atmosphere and Volatile Evolution (MAVEN) mission a good chance to observe magnetic fields and planetary ions' behavior simultaneously. Two years' MAVEN data show a reduced atmospheric ion escape above Martian Crustal Field region suggests magnetic field's protective effect on heavy planetary ions. The effective altitude of magnetic field's protective effect is from 400 km to 1800 km and reduces a maxim escape rate of 40 percent. Two physical mechanisms contribute to this protective effect which forms an upper limit and a lower limit of net O^+ fluxes. This is the first time directly shows Crustal Field's protective effect on heavy planetary ions. Since a locally small Crustal Field could protect its atmosphere and slow down solar wind erosion process, the protection of a planet's strong dipole field on escaping ions should be more effective. Planetary magnetic field may significantly affect a planet's climatic evolution and deeply changing the fate of extraterrestrial life.

EPSC Abstracts
Vol. 12, EPSC2018-707, 2018
European Planetary Science Congress 2018

First Global Model of Meteoric Magnesium in the Martian Atmosphere

John Plane (1), Francisco González-Galindo (2), Juan Diego Carrillo-Sánchez (1), Jean-Yves Chaufray (3), Francois Forget (4), Matteo Crismani (5), and Nicholas Schneider (5)
(1) School of Chemistry, University of Leeds, Leeds, UK, (2) Instituto de Astrofísica de Andalucía, CSIC, Granada, Spain, (3) Laboratoire Atmosphères, Milieux, Observations Spatiales, IPSL, Paris, France, (4) Laboratoire de Meteorologie Dynamique, Universite Paris VI, Paris, France, (5) Laboratory for Atmospheric and Space Physics, University of Colorado, Boulder, USA (j.m.c.plane@leeds.ac.uk)

Abstract

Meteoric ablation produces a layer of Mg^+ ions peaking around 90 km in the Martian atmosphere. The layer was recently recorded by NASA's MAVEN spacecraft, the first time that a meteoric metal layer has been observed directly in another planetary atmosphere. These metals are very useful tracers of chemistry and dynamics, as well as being significant components of the lower ionospheric plasma and forming nuclei for the condensation of mesospheric ice clouds. A module of Mg neutral and ion-molecules reactions, which have mostly been studied in the laboratory, were included in the Laboratoire de Météorologie Dynamique (LMD) Mars global circulation model to investigate the global Mg^+ and Mg layers. A simulation over a full Martian year reveals very surprising differences with the Mg^+/Mg layers in the terrestrial atmosphere, on diurnal, seasonal and latitudinal scales.

1. Introduction

The ablation of cosmic dust in planetary atmospheres produces a continuous injection of metallic vapours such as Mg, Fe and Na [1]. Although the metallic atoms and ions have been observed for four decades in the terrestrial atmosphere [8], it was only recently that meteoric metals have been observed directly in another planetary atmosphere. The Imaging Ultraviolet Spectrograph (IUVS) on NASA's Mars Atmosphere and Volatile EvolutioN (MAVEN) mission has observed the dayglow emission at 280 nm from Mg^+ ions. These ions occur as a layer in the Martian atmosphere between 70 and 130 km, peaking around 90 km with a peak density of ~350-400 cm^{-3} [2]. One surprising result is that a neutral Mg atom layer has not been detected by IUVS, despite a very good instrumental detection limit [2], in contrast to earlier model predictions [9]. We have recently used a 1-D model to show that the absence of Mg can be explained by the dissociative recombination of CO_2-clustered MgO^+ ions with electrons to form $MgCO_3$ directly, rather than Mg [7]. Figure 1 shows that satisfactory agreement with Mg^+ observations around midday at low latitudes was achieved. Furthermore, the Mg layer is just below the IUVS detection limit at 90 km. $MgCO_3$ has a very large electric dipole moment (11.6 Debye), and thus form clusters with up to 6 H_2O molecules at temperatures below 150 K. These clusters should then coagulate efficiently to form metal carbonate-rich ice particles which can act as nucleating particles for CO_2-ice clouds [7].

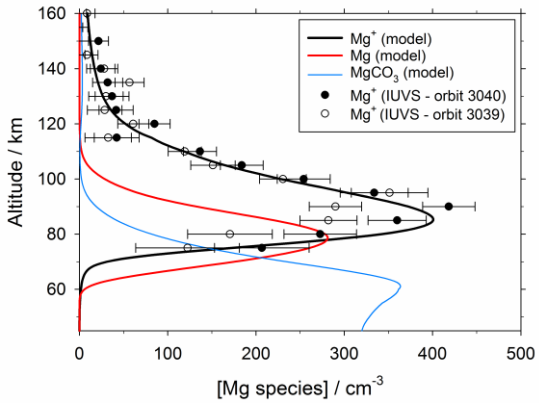

Figure 1: Vertical profiles of Mg^+, Mg and $MgCO_3$ predicted by the 1D model for local noon at the equator, $L_s = 85^o$. The symbols show Mg^+ measurements by the IUVS instrument during two successive orbits (reproduced from ref. [7]).

MAVEN's Neutral Gas Ion Mass Spectrometer (NGIMS) has measured a range of ions, including Mg^+, Fe^+ and Na^+ during deep dip orbits, which extend periapse down to 130 km [4]. These measurements have revealed several surprises: ions

of very different masses have the same scale heights above the homopause (i.e. there is limited gravitational separation), and often have the same scale height as the neutral atmosphere (i.e. ambipolar diffusion does not seem to dominate transport) [4].

2. The LMD-Mg model for Mars

The LMD Mars general circulation model extends from the surface to the exosphere, and has been developed for the self-consistent study of coupling between all layers of the atmosphere [3]. The version of the model used here includes an extension of the chemistry module to include nitrogen chemistry and ion-molecule chemistry relevant to the ionosphere, as well as improved treatments of the day-to-day variability of the UV solar flux and 15 μm CO_2 cooling under non-local thermodynamic equilibrium conditions [3].

A set of 22 Mg neutral and ion-molecule reactions, validated through the satisfactory fit to IUVS observations shown in Figure 1, were then added to the chemical model. The Meteoric Input Function (MIF) for Mg was calculated from the absolute fluxes of cosmic dust particles entering the Martian atmosphere from short-period Jupiter Family Comets, Long Period Comets and Asteroids [1]. The size and velocity distributions of dust from each source were determined from an astronomical model [6], and the height-dependent Mg ablation rate from individual particles was calculated using the Leeds Chemical Ablation Model (CABMOD) [1]. The total dust input rate is estimated to be 3.6 t sol^{-1}.

3. Results and Discussion

The LMD-Mg model has been run for a full Martian year. It should be noted that the Mg^+ and Mg layers in the terrestrial atmosphere have been observed near-globally between 70 and 140 km by the SCIAMACHY instrument onboard the Envisat satellite, and satisfactorily modelled using the Whole Atmosphere Community Climate (WACCM) model [5]. The terrestrial situation provides a useful contrast with Mars. Dynamics clearly controls the Martian Mg/Mg^+ layers much more strongly than in the Earth's atmosphere, producing quite unexpected diurnal, seasonal and latitudinal variations. These will be compared to IUVS observations.

Acknowledgements

This work is supported by the UK Science and Technology Facilities Council (ST/P00041X/1).

References

[1] Carrillo-Sánchez, J. D., Nesvorný, D., Pokorný, P., Janches, D., and Plane, J. M. C.: Sources of cosmic dust in the Earth's atmosphere, Geophys. Res. Lett., Vol. 43, pp. 11979-11986, 2016.

[2] Crismani, M. M. J., Schneider, N. M., Plane, J. M. C., Evans, J. S., Jain, S. K., Chaffin, M. S., Carrillo-Sanchez, J. D., Deighan, J. I., Yelle, R. V., Stewart, A. I. F., McClintock, W., Clarke, J., Holsclaw, G. M., Stiepen, A., Montmessin, F., and Jakosky, B. M.: Detection of a persistent meteoric metal layer in the Martian atmosphere, Nat. Geosci., Vol. 10, pp. 401–404, 2017.

[3] González-Galindo, F., Chaufray, J.-Y., López-Valverde, M. A., Gilli, G., Forget, F., Leblanc, F., Modolo, R., Hess, S., and Yagi, M.: Three-dimensional Martian ionosphere model: I. The photochemical ionosphere below 180 km, J. Geophys. Res. - Planets, Vol. 118, pp. 2105-2123, 2013.

[4] Grebowsky, J. M., Benna, M., Plane, J. M. C., Collinson, G. A., Mahaffy, P. R., and Jakosky, B. M.: Unique, non-Earthlike, meteoritic ion behavior in upper atmosphere of Mars, Geophys. Res. Lett., Vol. 44, 2017.

[5] Langowski, M. P., Savigny, C. v., Burrows, J. P., Feng, W., Plane, J. M. C., Marsh, D. R., Janches, D., Sinnhuber, M., Aikin, A. C., and Liebing, P.: Global investigation of the Mg atom and ion layers using, SCIAMACHY/Envisat observations between 70 and150 km altitude and WACCM-Mg model results, Atmos. Chem. Phys., Vol. 15, pp. 273–295, 2015.

[6] Nesvorný, D., Vokrouhlicky, D., Pokorný, P., and Janches, D.: Dynamics of dust particles released from Oort Cloud comets and their contribution to radar meteors, Astrophys. J., Vol. 743, pp. 12, 2011.

[7] Plane, J. M. C., Carrillo-Sánchez, J. D., Mangan, T. P., Crismani, M. M. J., Schneider, N. M., and Määttänen, A.: Meteoric Metal Chemistry in the Martian Atmosphere, J. Geophys. Res.-Planets, Vol. 123, pp. 695-707, 2018.

[8] Plane, J. M. C., Feng, W., and Dawkins, E. C. M.: The Mesosphere and Metals: Chemistry and Changes, Chem. Rev., Vol. 115, pp. 4497-4541, 2015.

[9] Whalley, C. L. and Plane, J. M. C.: Meteoric ion layers in the Martian atmosphere, Faraday Disc., Vol. 147, pp. 349-368, 2010.

EPSC Abstracts
Vol. 12, EPSC2018-940, 2018
European Planetary Science Congress 2018

Modelling Flux Ropes in the Ionosphere of Titan

C J Martin (1), C S Arridge (1), S V Badman(1), L C Ray(1), C T Russell (2), H Y Wei (2) and M K Dougherty (3)
(1) Department of Physics, Lancaster University, Bailrigg, Lancaster, UK (c.martin1@lancaster.ac.uk)

(2) IGPP, University of California LA, USA

(3) Blackett Laboratory, Imperial College, London UK

Abstract

Titan is Saturn's largest and most compelling moon. Its unique interaction with Saturn's magnetic field makes it a hotbed for the study of dynamic features such as flux ropes (bundles of twisted magnetic field). Titan itself has no intrinsic magnetic field, but as Saturn's magnetosphere rotates it builds up a draped magnetic field, very similar to Venus' interaction with the solar wind, which is `caught-up' in Titan's dense ionosphere. We use Cassini magnetometer data to detect flux ropes, and use a number of force-free and non-force-free models to examine the differences and similarities between these flux ropes and flux ropes found at other planetary ionospheres. We comment on how the presence of flux ropes in Titan's ionosphere are effected by the changing magnetic interaction we see at Titan. We also infer how the flux ropes may initiate and develop using Bayesian inference to show the different properties of each flux rope.

1. Introduction

Flux ropes are ubiquitous throughout the solar system and are bundles of magnetic field that have a strong axially aligned field at the center which becomes increasingly tangential with radius. Saturn's magnetic field is stretched outward at the equator due to centrifugal stresses [4] and flaps up and down with a number of periodicities [5,6]. As Titan orbits at Saturn's rotational equator just inside the magnetopause we find that Titan is exposed to a number of varying magnetic environments and as Titan has no intrinsic magnetic field of its own, but a very thick ionosphere and atmosphere, we find that Saturn's field is 'captured' by the ionosphere [7]. We use Cassini magnetometer [1] data to detect flux ropes in Titan's ionosphere by finding large peaks in magnetic field magnitude and use variance analysis to determine if the field shows a flux rope-like structure

2. Models

We test a number of models to determine the properties of the flux ropes, such as the radii, axial magnetic field (as we will rarely sample the center of the flux ropes) and the flux content of each one. The first model we will investigate is the force-free model [2]. This model is based upon the Bessel function solutions in cylindrical co-ordinates. The second model we will discuss in depth is the non-force-free Nieves-Chinchilla [3] model. This model does not assume that the JxB force in the flux rope is zero, and hence we fit for a polynomial expansion of the currents in the flux rope. Both models also assume that the flux rope is not bent and has a perfectly circular cross-section, we will further discuss the implications of a bending flux rope model as well as flux ropes with an elliptical cross section.

3. Results

We find that, through use of the two models discussed above, that the 85 flux ropes found at Titan are more suitably fitted to a non-force-free model than the force-free model. We also find that using a bent flux rope model will also effect the parameters that are given by the fitting and hence we show that the models may not give accurate values of radius and axial magnetic field if the flux rope is suspected to be in a bent or twisted configuration. Figure 1 shows a comparison of values found from both models, the distributions are built using kernel smoothing where each value has a mean (its value) and a standard deviation (its uncertainty) which makes a normal distribution peak. All of these normal distributions are added together to build the probability distribution shown. Further to this we will investigate all the

properties of the flux ropes using Bayesian inference to show the interdependence and improved error analysis of the parameters fitted to both models. The section below shows a typical example where the non-force-free model shows an improved fit (figure 2).

4. Figures

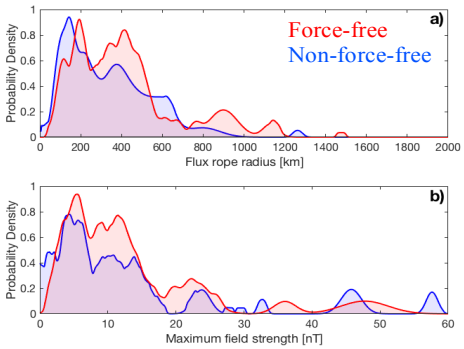

Figure 1: The comparison of values of radii (a) and axial field strength (b) of the force-free (red) and non-force-free (blue) models.

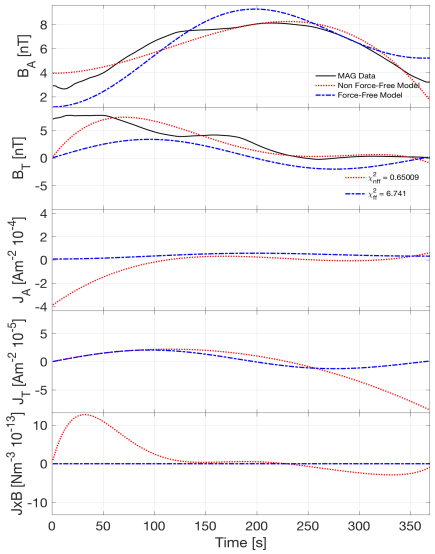

Figure 2: Figure shows a comparison between a non-force-free (red) model fit to a force-free (blue) model fit to data (black). The top two panels show magnetic field in the Axial and tangential directions and the bottom three show the currents expected from both models and the JxB force. Note how the JxB force of the force-free model is near zero.

5. Summary and Conclusions

We have discussed the highly dynamic and variable environments that Titan can be exposed to, and in these environments we find changing numbers of flux ropes. We hope to link the magnetic environment with the formation and development of flux ropes using Bayesian inference in the near future and show that Titan is an ideal environment for creating flux ropes, but not sustaining them. The use of both models discussed already show that the majority of flux ropes cannot be considered force-free and hence can be classed as 'non-matured' flux ropes.

References

[1] Dougherty, M. K., S. Kellock, D. J. Southwood, A. Balogh, E. J. Smith, B. T. Tsurutani, B. Gerlach et al. "The Cassini magnetic field investigation." In *The Cassini-Huygens mission*, pp. 331-383. Springer, Dordrecht, 2004.

[2] Lepping, R.P., Jones, J.A. and Burlaga,L.F.: Magnetic field structure of interplanetary magnetic clouds at 1 AU in Journal of Geophysical Research. Vol. 95 A8 (1990)

[3] Nieves-Chinchilla, Teresa, M. G. Linton, Miguel A. Hidalgo, Angelos Vourlidas, Neel P. Savani, Adam Szabo, Charlie Farrugia, and Wenyuan Yu. "A circular-cylindrical flux-rope analytical model for magnetic clouds." *The Astrophysical Journal* 823, no. 1 (2016): 27.

[4] Arridge, C. S., C. T. Russell, K. K. Khurana, N. Achilleos, S. W. H. Cowley, M. K. Dougherty, D. J. Southwood, and E. J. Bunce. "Saturn's magnetodisc current sheet." JGR: Space Physics 113, no. A4 (2008).

[5] Provan, G., David Jeremy Andrews, Chris S. Arridge, Andrew J. Coates, S. W. H. Cowley, G. Cox, M. K. Dougherty, and C. M. Jackman. "Dual periodicities in planetary-period magnetic field oscillations in Saturn's tail." Journal of Geophysical Research: Space Physics 117, no. A1 (2012).

[6] Arridge, Chris S., N. André, K. K. Khurana, C. T. Russell, S. W. H. Cowley, G. Provan, D. J. Andrews et al. "Periodic motion of Saturn's nightside plasma sheet." *Journal of Geophysical Research: Space Physics* 116, no. A11 (2011).

[7] Bertucci, C., N. Achilleos, M. K. Dougherty, R. Modolo, A. J. Coates, K. Szego, A. Masters et al. "The magnetic memory of Titan's ionized atmosphere." Science 321, no. 5895 (2008): 1475-1478.

EPSC Abstracts
Vol. 12, EPSC2018-951, 2018
European Planetary Science Congress 2018

An analytic model of comet ionosphere chemistry

Erik Vigren
Swedish Institute of Space Physics, Uppsala, Sweden (erik.vigren@irfu.se)

Abstract

We present an alternative approach for modeling ion-neutral chemistry in the inner coma of a low to moderately active comet [1]. The new model is analytic in its nature. Closed-form expressions to calculate fractional ion number densities as a function of cometocentric distance and activity level are presented. Advantages and limitations of the new method compared with the more standard approach of cometary ionosphere chemical modeling will be discussed.

References

[1] Vigren, E., Analytic model of comet ionosphere chemistry, A&A in print.

EPSC Abstracts
Vol. 12, EPSC2018-954, 2018
European Planetary Science Congress 2018

Temperature anisotropies of proton velocity distributions in the plasma environment of Venus

Alexander Bader (1,2,3), **Gabriella Stenberg Wieser** (1), Mats André (4), Martin Wieser (1), Yoshifumi Futaana (1), Moa Persson (1), Hans Nilsson (1) and Tielong Zhang (5)
(1) Swedish Institute of Space Physics, Kiruna, Sweden, (2) Luleå University of Technology, Luleå, Sweden, (3) Lancaster University, Lancaster, United Kingdom, (4) Swedish Institute of Space Physics, Uppsala, Sweden, (5) Space Research Institute, Austrian Academy of Science, Graz, Austria (gabriella@irf.se)

Abstract

Using data from Venus Express, we study proton velocity distributions in the plasma environment of Venus. We focus on temperature anisotropies, that is, the difference between the proton temperature parallel and perpendicular to the background magnetic field. We present a spatial map of the average ratio between the perpendicular and parallel temperatures, $T_\perp$ and $T_{||}$ in Venus plasma environment. Near the subsolar point the perpendicular heating is strongest, forming highly unstable proton velocity distributions in a hot and dense plasma. Such conditions are ideal for frequent mirror mode wave generation.

1. Introduction

Many different plasma wave types have been observed around Venus and it is well-known that wave-particle interaction is important for ion acceleration and ion escape processes at Earth [1], but how important are they at Venus? Ion escape is observed both by Pioneer Venus Orbiter and Venus Express and the total ion outflow from Venus is estimated to be in the range 10^{24}-10^{25} s^{-1} [2, 3].

A number of processes are able to remove ions from Venus' atmosphere: tailward acceleration in the plasma sheet by the magnetic tension force, magnetotail reconnection, and ion pickup and acceleration by the convection electric field. Our aim is to investigate observed proton velocity distribution functions (VDFs) in order to better understand the interplay between particles and waves and to judge the importance of wave-particle interaction for ion escape and other processes in the induced magnetosphere around Venus.

2. Data

The investigation is based on Venus Express data recorded from May 2006 to December 2009. We use ion data from the Ion Mass Analyzer (IMA), a sensor which is part of the ASPERA-4 instrument package [4] and magnetometer data with 4-s resolution from MAG [5].

3. Preliminary results

Figure 1 shows a map of the proton temperature ratio in the X_{VSO}-R_{VSO}-plane, where $R_{VSO} = \sqrt{Y_{VSO}^2 + Z_{VSO}^2}$. The VSO-system is centered on Venus, with X_{VSO} pointing towards the sun, Y_{VSO} opposite to the orbital motion and Z_{VSO} completing the righthand system by pointing northward, perpendicular to the orbital plane.

In the solar wind we observe temperature ratios very close to $T_\perp/T_{||} = 1$. This agrees well with [6], who found that the core distribution of solar wind protons at low and medium speeds is typically isotropic at Venus' radial distance from the Sun. In high-speed solar wind, pronounced anisotropies of $T_\perp/T_{||} > 1$ have been observed in the core distribution. As the number of VDFs measured at low to medium SW speeds greatly outweighs those at high speeds, we expect to obtain median values pointing to isotropic distributions.

The ratio $T_\perp/T_{||}$ increases at the bow shock, where some of the incident ions are reflected at the shock. In the subsolar compression region, where the interaction with Venus' induced magnetosphere is strongest, perpendicular temperature anisotropies with $T_\perp/T_{||} > 4/3$ can frequently be observed.

The proton distributions become more isotropic as the plasma flows downstream past Venus. This may be attributed to the generation of low-frequency waves which serve to transfer energy between different proton populations and stabilize the downstream distribu-

tions. In the magnetotail we instead observe a slight $T_\perp/T_{||} < 1$ anisotropy.

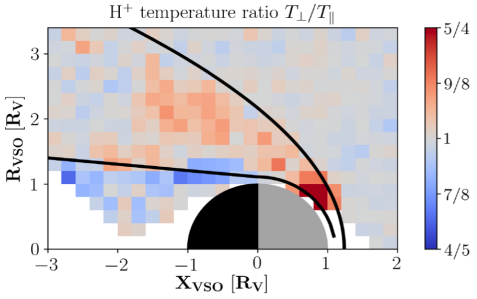

Figure 1: Proton temperature ratio $T_\perp/T_{||}$ around Venus in the X_{VSO}-R_{VSO}-plane. The colorscale has been adjusted such that for example a ratio of 3/2 is displayed in red with the same color intensity as its inverse value 2/3 in blue.

The observed proton bulk velocity together with the typical temperature ratio, $T_\perp/T_{||}$, in different regions around Venus is presented in the table below.

Table 1: Proton bulk velocity and temperature ratio in the solar wind, magnetosheath, magnetotail and subsolar compression region

	v_{bulk} [km/s]	$T_\perp/T_{\|\|}$ ratio
Solar wind	409±14	1.00
Magnetosheath	351±19	1.02
Magnetotail	73±22	0.98
Subsolar region	201±3	1.36

4. Conclusions

We observe highly isotropic proton distributions upstream of the bow shock. Upon passing the bow shock, the protons are heated and the heating is more pronounced in directions perpendicular to the magnetic field. The VDFs in the magnetosheath are therefore slightly anisotropic with $T_\perp > T_{||}$. In the dayside magnetosheath where the compression of Venus' induced magnetosphere is strongest, the heating is strongly increased compared to the rest of the magnetosheath. Pronounced temperature anisotropies with on average $T_\perp/T_{||} \approx 4/3$ are a clear signature of plasma distributions unstable to low frequency wave generation. The instability criterion for mirror mode waves is found to be frequently fulfilled in this region, which agrees well with previous waves observations reported by [7, 8].

References

[1] André, M. & Yau, A. Theories and Observations of Ion Energization and Outflow in the High Latitude Magnetosphere, Space Science Reviews, 80 (1-2), 27-48, 1997.

[2] Russell, C., J. Luhmann, and R. Strangeway, The solar wind interaction with venus through the eyes of the pioneer venus orbiter, Planetary and Space Science, 54 (13), 1482-1495, 2006.

[3] Nordström, T., G. Stenberg, H. Nilsson, S. Barabash, and T. Zhang, Venus ion outflow estimates at solar minimum: Influence of reference frames and disturbed solar wind conditions, Journal of Geophysical Research: Space Physics, 118 (6), 3592-3601, 2013.

[4] Barabash, S., et al., The analyser of space plasmas and energetic atoms (ASPERA-4) for the Venus express mission, Planetary and Space Science, 55 (12), 1772-1792, 2007.

[5] Zhang, T., et al., Magnetic field investigation of the Venus plasma environment: Expected new results from Venus Express, Planetary and Space Science, 54 (13), 1336-1343, 2006.

[6] Marsch, E., K.-H. Mühlhäuser, R. Schwenn, H. Rosenbauer, W. Pilipp, and F. Neubauer, Solar wind protons: Three-dimensional velocity distributions and derived plasma parameters measured between 0.3 and 1 au, Journal of Geophysical Research: Space Physics, 87 (A1), 52-72, 1982.

[7] Volwerk, M., T. Zhang, M. Delva, Z. Vörös, W. Baumjohann, and K.-H. Glassmeier, First identification of mirror mode waves in Venus' magnetosheath?, Geophysical Research Letters, 35 (12), 2008.

[8] Volwerk, M., D. Schmid, B. Tsurutani, M. Delva, F. Plaschke, Y. Narita, T. Zhang, and K.-H. Glassmeier, Mirror mode waves in venus's magnetosheath: solar minimum vs. solar maximum, in Annales Geophysicae, vol. 34, p. 1099, Copernicus GmbH, 2016.

EPSC Abstracts
Vol. 12, EPSC2018-964, 2018
European Planetary Science Congress 2018

Observations of a Solar Energetic Particle event from inside the comet 67P coma and upstream of the comet

Anne Wellbrock (1,2), Geraint H. Jones (1,2), Andrew J. Coates (1,2), Cyril Simon Wedlund (3), Charlotte Goetz (4), Nina Dresing (5), Tom A. Nordheim (6), Kathy E. Mandt (7), Rajkumar Hajra (8), Minna Myllys (8), Pierre Henri (8), and Hans Nilsson (9)

(1) Mullard Space Science Laboratory, University College London, UK, (2) The Centre for Planetary Sciences at UCL/Birkbeck, UK, (3) University of Oslo, Norway, (4) TU Braunschweig, Germany, (5) University of Kiel, Germany, (6) NASA JPL, California, USA, (7) APL, John Hopkins University, Maryland, USA, (8) CNRS, France, (9) IRF Kiruna, Sweden (a.wellbrock@ucl.ac.uk)

Abstract

We used ESA's Standard Radiation Environment Monitors (SREM) on-board Rosetta to identify a number of Solar Energetic Particle (SEP) events from inside the comet 67P's coma. In this study we focus on one of these which was observed at Rosetta on 7 March 2015 at a perihelion distance of 2.15AU and a cometocentric distance of about 70km. We show observations of the SEPs and associated events upstream of the comet by other spacecraft such as STEREO and SOHO. The SEPs appear to be linked to a CME and flare observed at the Sun on 6 March 2015. We also show other Rosetta data, such as from RPC (Rosetta Plasma Consortium), in order to study and discuss the effects of the SEPs on the comet's coma.

EPSC Abstracts
Vol. 12, EPSC2018-993-2, 2018
European Planetary Science Congress 2018

Low energy ion measurements at comet 67P

Fredrik L. Johansson (1,2), Elias Odelstad (1,2), Anders Eriksson (1), Erik Vigren (1), Pierre Henri (3)
(1) Swedish Institute of Space Physics, Uppsala, Sweden, (2) Uppsala University, Sweden (frejon@irfu.se), (3) Laboratoire de Physique et Chimie de l'Environnement et de l'Espace, CNRS, Orléans, France

Abstract

ESA Rosetta spacecraft studies of the 67P/Churyumov-Gerasimenko coma indicate the presence of an electric field capable of accelerating the cometary ions a factor of 2-10 times the neutral gas outgassing velocity and thus a decoupling of the cometary ions from the neutrals. The plasma instrumentation on-board Rosetta in the Rosetta Plasma Consortium (RPC) are all in situ measurements taken on an often significantly negatively charged spacecraft ($\approx$ -10 to -30 V) capable of perturbing ion measurements. Therefore simulations of the Spacecraft-plasma interaction were undertaken with the Spacecraft-Plasma Interaction System code (SPIS) to investigate the features and extent of this perturbation. In this study we report preliminary results of positive ion measurements using simulated voltage-bias sweeps of the Rosetta Langmuir Probes (RPCLAP), with varying random and ram flow velocity components, indicate a non-negligible decrease of ion flux to the probe with increasingly negative spacecraft potential. We also show that this spacecraft-plasma interaction effect would rarely be sufficient to return to an ion-neutral coupled environment model for typical Rosetta plasma observations.

1. Introduction

ESA's comet-chaser Rosetta arrived at comet 67P/Churyumov-Gerasimenko in August 2014 and completed its mission in September 2016. During all this time, the instruments of the Rosetta Plasma Consortium (RPC) were monitoring the plasma environment. The Langmuir probe instrument (RPC-LAP) [1], measures the current between the probe and surrounding space with the aim to characterise the plasma.

Previous simulations [2, 6, 5] show that a proper interpretation of the plasma measurements on Rosetta need to take spacecraft potential effects into account, as electrons and ions are attracted or repelled towards the spacecraft, as shown in Figure 1. The extent of which we attempt to quantify and study in this report with further, more detailed simulations focused on a comet-like environment using *Spacecraft-Plasma Interaction System* (SPIS) [4].

2. Method and Results

For supersonic ion flow of single positive charge, the ion current to a sphere such as the Rosetta Langmuir Probe can be shown[3] to be

$$I_i = \begin{cases} -I_{i0}\left(1 - \frac{eV_p}{E_i}\right) & \text{for } V_p < E_i/e \\ 0 & \text{for } V_p > E_i/e, \end{cases} \quad (1)$$

where V_p is the absolute potential of the probe relative to a plasma at infinity, e is the elementary charge, $E_i = \frac{m_i u^2}{2}$ is the energy of ions of mass m_i, and flow speed u, I_{i0} is the ram current, given by

$$I_{i0} = A_c e n u, \quad (2)$$

where A_c is the circular cross section of the probe, n is the plasma density. For typical cometary plasma as seen by Rosetta, I_{i0} is below the measurement resolution of RPCLAP [1] of 0.3 nA. Therefore we instead use the derivative of the ion current $\frac{dI_i}{dV_p}$ and plasma density estimates from RPC-MIP [7] to estimate the ion flow speed.

We can also obtain a second estimate the effective ion flow speed by a method proposed by Vigren et al. (2017) [8] using a simple flux conservation model assuming radial outflow. The results are plotted in Figure 2, at times where the outgassing velocity is just below 1 km/s. We have conducted nine simulated Langmuir Probe voltage-bias sweeps of a nominal case event study, with varying components of thermal and flow velocity to determine the degree of perturbation due to the presence of a highly negative spacecraft in SPIS, and found that the ion flux to the probe decrease by a factor of 1.5 to 2, which would result in the mean of the LAP ion slope method result approaching 2-3

km/s, much in agreement with the flux conservation method, but still above the neutral gas flow speed.

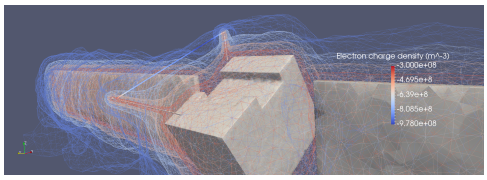

Figure 1: Electron density profile surrounding a -20 V charged Rosetta spacecraft model used in the simulations.

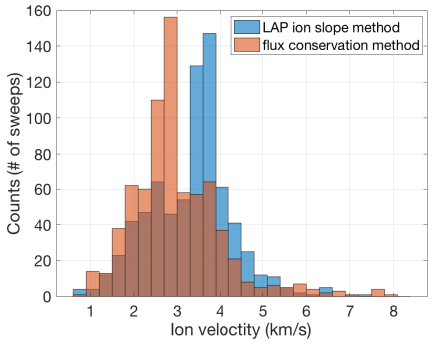

Figure 2: Comparison of effective ion drift speeds obtained from the flux conservation model [8] and the LAP ion slope method during all diamagnetic cavity crossings throughout the mission.

Acknowledgements

Rosetta is a European Space Agency (ESA) mission with contributions from its member states and the National Aeronautics and Space Administration (NASA). Support by the Swedish National Space board is acknowledged, including SNSB contracts 109/12, 135/13, 166/14 and 168/15.

References

[1] A. I. Eriksson, R. Boström, R. Gill, L. \AAhlén, S.-E. Jansson, J.-E. Wahlund, M. André, A. Mälkki, J. A. Holtet, B. Lybekk, A. Pedersen, and L. G. Blomberg. RPC-LAP: The Rosetta Langmuir Probe Instrument. *Space Sci. Rev.*, 128:729–744, Feb. 2007.

[2] A. I. Eriksson, C. H\a anberg, and A. Sjögren. Modeling of spacecraft potential measurements on Rosetta. In *Proceedings of the 11th Spacecraft Charging Technology Conference (SCTC-11), NASA*, 2010.

[3] U. Fahleson, C. G. Fälthammar, and A. Pedersen. Ionospheric temperature and density measurements by means of spherical double probes. *Planetary and Space Science*, 22(1):41–66, Jan. 1974.

[4] J.-C. Matéo-Vélez, P. Sarrailh, B. Thiébault, J. Forest, A. Hilgers, J.-F. Roussel, G. Dufour, B. Rivière, V. Génot, S. Guillemant, A. Eriksson, C. Cully, and D. Rodgers. SPIS Science: modelling spacecraft cleanliness for low-energy plasma measurement. *12th Spacecraft Charging Technology Conf. Kitakyushu, Japan*, May 2012.

[5] J. Olson, N. Brenning, J.-E. Wahlund, and H. Gunell. On the interpretation of Langmuir probe data inside a spacecraft sheath. *Review of Scientific Instruments*, 81(10):105106–105106, Oct. 2010.

[6] J.-F. Roussel and J.-J. Berthelier. A study of the electrical charging of the Rosetta orbiter: 1. Numerical model. *Journal of Geophysical Research (Space Physics)*, 109:A01104, Jan. 2004.

[7] J. G. Trotignon, J. L. Michau, D. Lagoutte, M. Chabassière, G. Chalumeau, F. Colin, P. M. E. Décréau, J. Geiswiller, P. Gille, R. Grard, T. Hachemi, M. Hamelin, A. Eriksson, H. Laakso, J. P. Lebreton, C. Mazelle, O. Randriamboarison, W. Schmidt, A. Smit, U. Telljohann, and P. Zamora. RPC-MIP: the Mutual Impedance Probe of the Rosetta Plasma Consortium. *Space Science Reviews*, 128(1):713–728, 2006.

[8] E. Vigren, M. André, N. J. T. Edberg, I. a. D. Engelhardt, A. I. Eriksson, M. Galand, C. Goetz, P. Henri, K. Heritier, F. L. Johansson, H. Nilsson, E. Odelstad, M. Rubin, G. Stenberg-Wieser, C.-Y. Tzou, and X. Vallières. Effective ion speeds at ∼200–250 km from comet 67p/Churyumov–Gerasimenko near perihelion. *Monthly Notices of the Royal Astronomical Society*, 469(Suppl_2):S142–S148, July 2017.

EPSC Abstracts
Vol. 12, EPSC2018-1075-1, 2018
European Planetary Science Congress 2018

Plasma waves near the diamagnetic cavity of comet 67P

Elias Odelstad (1,2), Anders Eriksson (1), Tomas Karlsson (3), Hugo Breuillard, (4), Charlotte Goetz (5) and Pierre Henri (4)
(1) Swedish Institute of Space Physics, Uppsala, Sweden (elias.odelstad@irfu.se), (2) Uppsala University, Uppsala, Sweden, (3) KTH Royal Institute of Technology, Stockholm, Sweden (4) LPC2E, CNRS, Orléans, France (5) TU Braunschweig, Braunschweig, Germany

Abstract

We report the detection of large-amplitude, quasi-harmonic density-fluctuations with associated magnetic field oscillations in the region surrounding the diamagnetic cavity of comet 67P. Typical frequencies are ∼0.1 Hz and there is a ∼90° phase lag between density and magnetic field fluctuations. We speculate that these are possibly dissipative waves associated with the steepened structures surrounding the diamagnetic cavity.

1. Observations

The region surrounding the cavity is characterized by steepened plasma density (Fig. 1a, left-hand y-axis) and magnetic field (Fig. 1b) enhancements. Large-amplitude, quasi-harmonic waves at ∼0.1 Hz appear in the the Langmuir probe (RPC-LAP) fixed-bias ion current (a high time resolution proxy for the plasma density, Fig. 1a, right-hand y-axis), typically coincident with these structures (blue ellipses in Fig. 1a). A zoom-in in Fig. 1c (of the green rectangle in Fig. 1a) reveals that these waves are indeed observed also in the Mutual Impedance Probe (RPC-MIP) plasma density measurements and that their relative amplitude is $\delta n/n \gtrsim 1$. The waves also come through in the magnetic field, though with a much lower relative amplitude. A further zoom-in in Fig. 1d (of the black rectangle in Fig. 1c) of highpass-filtered B-field (y-component) overplotted on the LAP current reveals a phase lag of ∼90° of the B-field w.r.t. the density fluctuations. A spectrum of the LAP current measurements during this brief snapshot exhibits a clear peak, in this case at ∼80 mHz.

2. Conclusions

The typical frequencies of the observed waves of ∼0.1 Hz is in the same neighbourhood as the "singing comet waves" [1]. However, those waves have been reported to disappear during the high-activity phase of the comet. Their suggested generation mechanism also does not work in this region [2]. Finally, the ∼90° phase lag of the magnetic field observed here differs from the typically observed phases of 0° or 180° of the "singing comet waves". Thus, we conclude that the herein presented wave observations constitute the detection of a new type of plasma waves at the comet, possibly dissipative waves associated with the steepened structures surrounding the diamagnetic cavity. Further work is required to investigate their prevalence at other times and examine their polarization properties.

References

[1] Richter, I., et al.: Observation of a new type of low-frequency waves at comet 67P/Churyumov-Gerasimenko, Ann. Geophys., 33, 1031-1036, Vol. 1, pp. 1-100, 2015.

[2] Meier, P.: Modified Ion-Wiebel Instability as a possible source of of low-frequency waves observed as 67P/Churyumov-Gerasimenko, Ann. Geophys., 34, 691-707 2016.

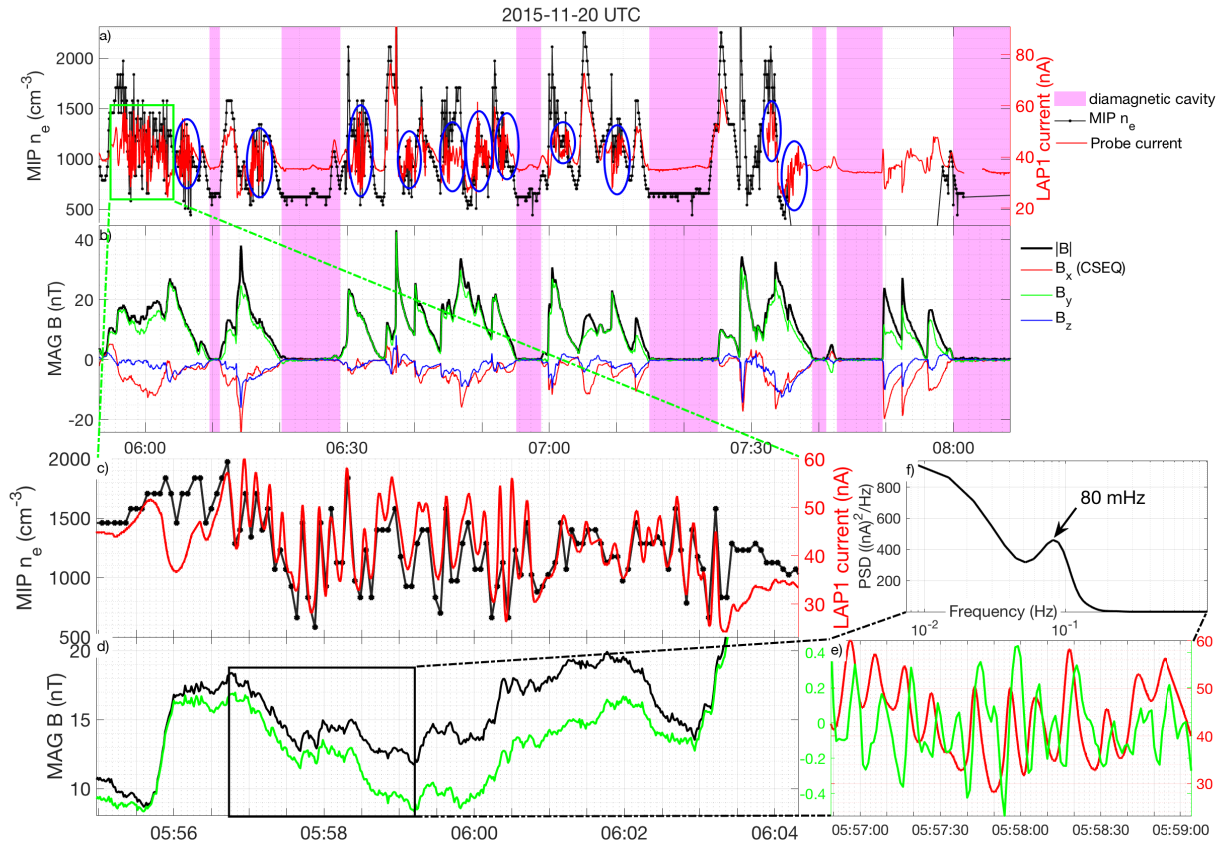

Figure 1: Wave observations near the diamagnetic cavity on Nov 20, 2015. a) MIP plasma density and LAP probe current, b) magnetic field, c-d) zoom-in from panels a-b, e) further zoom-in on LAP current (red) and highpass-filtered B-field (green), f) spectrum of LAP current in panel e.

EPSC Abstracts
Vol. 12, EPSC2018-1094, 2018
European Planetary Science Congress 2018

Cold Electrons at Comet 67P

Anders Eriksson (1), Ilka Engelhardt (1,2), Erik Vigren (1), Fredrik Johansson (1,2), Elias Odelstad (1,2), Niklas Edberg (1), Pierre Henri (3), Nicolas Gilet (3) and Martin Rubin (4)
(1) Swedish Institute of Space Physics, Uppsala (anders.eriksson@irfu.se), (2) Uppsala University, Sweden, (3) LPC2E, Universite d'Orléans, France, (4) University of Bern, Switzerland

Abstract

We present observations of cold (around or below 0.3 eV) in the coma of comet 67P covering all the Rosetta mission. While cold electrons were most abundant around perihelion (1.25 AU), we show their existence as far out as 3 AU. To explain the observations at low activity, we suggest that this is an effect of the ambipolar electric field keeping the electrons close to the nucleus and therefore give them time to cool on the neutrals.

EPSC Abstracts
Vol. 12, EPSC2018-1176, 2018
European Planetary Science Congress 2018

Observations of mixed warm and cold electrons with RPC-MIP at comet 67P/Churyumov-Gerasimenko

N. Gilet (1), P. Henri (1), A. I. Eriksson (2), X. Vallières (1), G. Wattieaux (3), C. Goetz (4), J. Moré (1), O. Randriamboarison (1), E. Odelstad (2,5) and F.L. Johansson (2,5)

(1) LPC2E-CNRS, ORLEANS CEDEX2, France (ngilet@cnrs-orleans.fr) (2) Swedish Institute of Space Physics, Uppsala, Sweden (3) Université de Toulouse, LAPLACE-UMR 5213, Toulouse, France (4) Institut für Geophysik und extraterrestrische Physik, TU Braunschweig, Braunschweig, Germany (5) Department of Physics and Astronomy, Uppsala University, Sweden

Abstract

In the ionosphere of the comet 67P/Churyumov-Gerasimenko, the Rosetta Plasma Consortium (RPC) instruments measured the plasma environment during more than two years from August 2014 to September 2016. The Ion Electron Sensor (RPC-IES) and the Langmuir Probes (RPC-LAP) reported different electron populations: (i) a suprathermal electron component (40-100 eV), (ii) a warm electron component of cometary origin (5-10 eV) and (iii) a cold component (<1 eV) of electrons thermalized by collisions with neutrals.

The Mutual Impedance Probe (RPC-MIP) has been operated to measure the total electron density. Gilet et al. [1] simulated the mutual impedance response for a probe immerged in a two-electron temperature plasma, with both cold and warm component were modelled by a Maxwellian distributions.

Through a direct comparison between simulated and observed mutual impedance spectra, the density and the temperature of the two electron populations have been retrieved for Rosetta data. This study focuses on three events: (i) on 2015 November 1 in the magnetized cometary plasma near perihelion (1.4 AU), (ii) inside a diamagnetic (unmagnetized) region on 2015 November 20, still near perihelion, and (iii) far from perihelion (3.2 AU) on 2016 May 23.

We illustrate the dynamics of the cold and warm electron populations and that the cold electrons can be transported along the magnetic field far from the electron-neutral collision region where the electrons are expected to have cooled down.

Acknowledgements

This work was supported by CNES and by ANR under the financial agreement ANR-15-CE31-0009-01. We acknowledge the financial support of label ESEP (Exploration Spatiale des Environnements Planétaires). The authors benefited from the use of the cluster Artemis (CaSciModOT) at the Centre de Calcul Scientifique en région Centre-Val de Loire (CCSC). Part of this work was inspired by discussions within International Team 402: "Plasma Environment of Comet 67P after Rosetta" and International Team 336: "Plasma Surface Interactions with Airless Bodies in Space and the Laboratory" at the International Space Science Institute, Bern, Switzerland. The Rosetta RPC-MIP mutual impedance spectra are publicly available on the ESA Planetary Science Archive (PSA).

References

[1] Gilet, N., Henri, P., Wattieaux, G., Cilibrasi, M., & Béghin, C. (2017). Electrostatic potential radiated by a pulsating charge in a two-electron temperature plasma. *Radio Science*, 52, 1432–1448.

.